



#### This is to certify that the

#### thesis entitled

Dynamic Flow Study in a Catalytic Converter using Laser Doppler Velocimetry and High Speed Flow Visualization

presented by

Kwang Sup Hwang

has been accepted towards fulfillment of the requirements for

M.S degree in Mechanical Eng.

Aurild J. Shruh

Major professor

Date\_\_\_\_June 16 1995

MSU is an Affirmative Action/Equal Opportunity Institution

**O**-7639

# LIBRARY Michigan State University

PLACE IN RETURN BOX to remove this checkout from your record.

TO AVOID FINES return on or before date due.

| DATE DUE         | DATE DUE | DATE DUE |
|------------------|----------|----------|
| MAY 0 9 1887     |          |          |
| MIN 0 9 1991     |          |          |
| July 21 01 20000 |          |          |
|                  |          |          |
|                  |          |          |
|                  |          |          |
|                  |          |          |

MSU is An Affirmative Action/Equal Opportunity Institution chickdesidus.pm3-p.1

# DYNAMIC FLOW STUDY IN A CATALYTIC CONVERTER USING LASER DOPPLER VELOCIMETRY AND HIGH SPEED FLOW VISUALIZATION

by

**Kwang Sup Hwang** 

#### **A THESIS**

Submitted to

Michigan State University
inpartial fulfillment of the requirements
for the degree of

**MASTER OF SCIENCE** 

Department of Mechanical Engineering

1995

#### **ABSTRACT**

# DYNAMIC FLOW STUDY IN A CATALYTIC CONVERTER USING LASER DOPPLER VELOCIMETRY AND HIGH SPEED FLOW VISUALIZATION

by

# **Kwang Sup Hwang**

Internal flow characteristics of a close-coupled, catalytic converter were examined by LDV measurements and high speed flow visualization. Although previous studies have been done on catalytic converters, most were conducted at steady state, using water flow that was seeded with a small quantity of tracer particles. The purpose of this study was to develop a better understanding of dynamic flows inside catalytic converters.

A Hyundai 4-cylinder engine head was fitted with standard exhaust valves, intake and exhaust manifolds, constant volume cylinders with no pistons, and full-open intake ports to simulate actual engine operation. Air and seed particles were forced through the system by a blower while an electric motor drove the cam. A clear- plastic, catalytic converter assembly

was connected to the exhaust manifold of the engine head, allowing optical access for the flow visualization and LDV. Measurements were conducted at two air flow/engine speed conditions: 120 standard cubic meters per hour (scmh) at 1000 rpm and 205 scmh at 2000 rpm. Two locations were chosen for the LDV measurements: 2.5 cm above the first catalyst brick and inbetween the first and second catalyst bricks. Flow visualization was also taken on two planes: along the major axis and parallel to the minor axis of the converter. Both planes are located at the inlet plenum, right above the first catalyst brick.

The high speed flow visualization films and LDV results showed that areas of separation and circulation were present in the inlet region of the converter. Backflows into the neck of the converter were also observed. Each cylinder exhausted into a different region of the converter, with the front-middle region having the heaviest amount of flow. High shear flows were created by each cylinder, while other regions of the inlet region showed backflows or recirculation. The midsection of the converter had a more uniform overall flow pattern than did the inlet section of the converter.

This thesis is dedicated to my brother,

Yong-Joon Hwang

( 1961-1986)

#### **ACKNOWLEDGMENTS**

I would like to take this opportunity to thank several people whose help and guidance made this work possible. First, my advisor Dr. Harold Schock for his support and guidance; to Dr. Keunchul Lee for his patience of teaching me the operation of LDV and also for making working at the MSU Engine Research Lab more enjoyable; John Mueller for having someone to work with the LDV, Dr. Craig Somerton and Dr. Mei Zhuang for being on my committee and giving me helpful comments; and to Tom Stuecken for his help in designing and building the test rig.

I also would like to express my gratitude to Hyundai Motor

Corporation for their financial support.

Finally I would like to thank my parents, Byungtai and Moonhwa Hwang for their continuous support during my graduate studies.

# **TABLE OF CONTENTS**

| Page  |
|---|
| LIST OF FIGURESviii                           |
| LIST OF SYMBOLSx                              |
| CHAPTER 1 - INTRODUCTION1                     |
| 1.1 Current Situation1                        |
| 1.2 Research Motivation3                      |
| CHAPTER 2 - EXPERIMENTAL FACILITIES5          |
| 2.1 Test Rig5                                 |
| A. Engine Head and Cylinder Assembly5         |
| B. Plastic Catalytic Converter6               |
| C. Flow System7                               |
| D. Electric Motor and Angle Encoder8          |
| E. External Lubrication System8               |
| 2.2 High Speed Flow Visualization(HSFL)10     |
| A. Seeding Particles for Flow Visualization10 |
| B. HSFV Hardware14                            |
| 2.3 Laser Doppler Velocimetry (LDV)16         |

|                | A. Seeding Particles for LDV      | 16  |
|----------------|-----------------------------------|-----|
|                | B. LDV Hardware                   | 17  |
| 2.             | .4 Computer Animation             | 21  |
| CHAPTER 3 - EX | XPERIMENTAL PROCEDURE             | 23  |
| 3.             | .1 Coordinate System              | 23  |
| 3.             | .2 Experimental Procedure         | 24  |
| 3.             | .3 Quantitative Measurement       | 24  |
| 3.             | .4 Flow Visualization             | 28  |
| CHAPTER 4 - RI | ESULTS AND DISCUSSIONS            | 31  |
| 4.             | .1 Exhaust Manifold Consideration | 31  |
| 4.             | .2 Flow Visualization Results     | 32  |
| 4.             | .3 LDV Results                    | 33  |
| CHAPTER 5 - CO | ONCLUSION AND RECOMMENDATION      | 41  |
| LICT OF DEED   | ENCES                             | 4.4 |

# **LIST OF FIGURES**

| Page   |
|--|
| Figure 1 Photograph of the test bench46                                      |
| Figure 2 Schematic of the test system47                                      |
| Figure 3 Photograph of the clear plastic assembly48                          |
| Figure 4 Photograph of the plastic cylinder assembly on the test stand48     |
| Figure 5 Photograph of the two piece converter49                             |
| Figure 6 Photograph of the assembled converter49                             |
| Figure 7 Photograph of the 3 hp DC electric motor50                          |
| Figure 8 Photograph of the angle encoder50                                   |
| Figure 9 Schematic of external oil supply system51                           |
| Figure 10 Schematic of the microballoon seeder51                             |
| Figure 11 Microballoon seeder illustrating (a) bypass flow, (b) flow through |
| the container and (c) throttled flow containg air and                        |
| seed52   |
| Figure 12 Schematic of the flow visualization system53                       |
| Figure 13 Schematic of the LDV system54                                      |
| Figure 14 Upper one component two beam system55                              |

| Figure 15 Lower two component 4 beam system55                               |
|---|
| Figure 16 Photograph of the fiberoptic probe mounted vertically on the test |
| rig56   |
| Figure 17 Coordinate systmem and axes description for the catalytic         |
| converter57   |
| Figure 18 Schematic of four flow visualization planes58                     |
| Figure 19 Schematic of intake and exhaust valve timing59                    |
| Figure 20 Sketches of flow patterns from the flow visualization films60     |
| Figure 21 Photograph of the catalytic converter and the wire mesh model61   |
| Figure 22 The location of six points in the inlet plenum62                  |
| Figure 23 W- velocity vs. crank angle at low flow rate63                    |
| Figure 24 Animated inlet plane velocity profile with 120 scmh flow rate at  |
| engine speed 1000 rpm64   |
| Figure 25 Animated midsection plane velocity profile with 120 scmh flow     |
| rate at engine speed 1000 rpm66   |
| Figure 26 Animated inlet plane velocity profile with 205 scmh flow rate at  |
| engine speed 2000 rpm68   |
| Figure 27 Animated midsection plane velocity profile with 205 scmh flow     |
| rate at engine speed 2000 rpm70   |

# **LIST OF SYMBOLS**

| τ                   | particle relaxation time                        |
|---------------------|---|
| Т                   | Lagrangian macro time scale of turbulence       |
| $\rho_p$            | particle density                                |
| $d_p$               | particle diameter                               |
| η                   | average gas viscosity                           |
| ε                   | momentum eddy diffusivity                       |
| v' <sup>2</sup>     | turbulence intensity                            |
| μ                   | turbulence viscosity                            |
| $d_p$               | finge spacing                                   |
| t1                  | time taken for the particles to cross the finge |
| F                   | Doppler shift frequency of scattered light      |
| λ                   | wavelength of the laser light                   |
| κ                   | half angle between beams                        |
| U(t)                | Instantaneous velocity                          |
| U(t)                | mean velocity                                   |
| $U_{\it EA(	heta)}$ | ensamble averaged mean velocity                 |
| u'ea (θ)            | ensemble average fluctuation                    |
|                     |   |

| Nc | number of cycle |
|----|-----------------|
| θ  | crank angle     |
| i  | cycle number    |

#### CHAPTER 1

#### INTRODUCTION

#### 1.1 Current Situation

Monolithic catalytic converter systems have been demonstrated to enable automobile manufacturers to comply with the Federal emission standards as specified in the Clean Air Act Amendment of 1970. However, the emission standards have been rising; not only the United States but the governments around the world as well Automotive manufacturers now face a problem of further reducing emissions and keeping the cost down as well. The catalytic converter has pronunced to be an excellent device to remove harmful exhaust gases before they reach the atmosphere. The catalytic converter used in spark-ignition engines consist of an active catalytic material in a specially designed metal enclosures that direct the exhaust gases throughout the catalyst bed. The active material employed for CO and HC oxidation or NO reduction must be distributed over a large surface area so that the mass-transfer characteristics between the gas phase and the active catalyst surface are sufficient to allow close to 100 percent conversion with high catalytic activity.

Little has been published relating to catalytic converter velocity distributions and practical means to improve flow mal-distributions. Previous studies done by Wendland and Matthes [1-3] were conducted on a steady flow-field using water flow seeded with a small quantity of tracer particles Lemme and Givens [4] measured the velocity with a small diameter pitot tube near the monolith exit face. Howitt and Sekella [5] measured flow velocity in round cross-section monolith converter using hot-wire anemometer and air as the working fluid. The flow field was found to be extremely maldistributed, with velocities decreasing with increasing distance from centerline.

Normally, the working fluid has been air or water. The advantage of using air is that it allows one to perform studies over a wide speed range. However, difficulties arise with seeding air because of its poor light scattering abilities makes it difficult for use with LDV and flow visualization.

Water analog models allow for the use of a larger seed than when using air. Larger particles scatter more light, which greatly facilitates flow visualization and LDV measurements. When a water analog is used, one must ensure that dynamic similitude is preserved. If boundary conditions are not exactly preserved, the flow results can be altered.[6] By creating a

uniform flow distribution, the lifetime of the converter would be increased and/or a smaller converter could be used.

#### 1.2 Research Motivation

The amount of exhaust flow produced by an engine determines the size of the catalyst brick needed in the catalytic converter. Maximum use of the catalyst volume is needed to maintain a high catalytic converter efficiency. To increase the active surface area, a uniform flow distribution across the active element is important. This results in the ability to use a smaller catalytic converter with uniform flow as opposed to a larger converter required for non-uniform flow. Use of non-uniform flow will result in an overuse of the areas that receive high flow volumes and underuse of low flow volumes. Thus, having uniform flow with a small converter will be more cost effective than the larger one with non-uniformity.

The purpose of this study was to characterize the flow patterns in a catalytic converter under normal engine operating conditions. This will lead to a better understanding of the internal flows in the catalytic converter. The effects of the exhaust manifold geometry and the angle of the diffuser at the inlet of the converter have a significant effect on the flow characteristics.

To gain complete optical access of the inside of the converter, a clear plastic converter was built. In understanding the complex flow fields, high speed flow visualization was employed in various planes of the converter. An LDV measurement is then applied to quantify the velocity field of interest. Measurements were conducted at two regions: the inlet plenum (2.5 cm in front of the first catalyst brick) and the midsection (between the catalyst bricks) of the catalytic converter. The flow rates used for the studies were 120 standard cubic meters per hour (scmh) at an engine speed of 1000 rpm and 205 scmh at an engine speed of 2000 rpm. The flow visualization films were taken at two perpendicular planes in the inlet plenum, for two different flow rates at a film speed of 5000 frames per second (fps). Velocity profile animation was created from the measured velocity vectors to examine the flow patterns through the catalytic converter. This technique allows for the comparison of the ensemble-averaged velocity profiles from LDV measurements to the cycle-resolved velocity patterns from the flow visualization films.[7] The results will be used for future designs of an improved converter.

#### CHAPTER 2

#### **EXPERIMENTAL FACILITIES**

# 2.1Test Rig

In this experiment the converter was placed on a test bench consisting of a blower, laminar flow meter, engine head with production intake and exhaust manifolds, and exhaust system. The picture of the test bench is shown in Figure 1 and the schematic of the test system on Figure 2.

# A. Engine Head and Cylinder Assembly

The 16 valve 4 cylinder engine head used in this experiment was modified to simulate the normal operating exhaust flow with steady air flow supplied by a blower. Modifications were minimized to preserve the characteristics of the engine operation. To reduce the complexity of having an actual engine and to gain better optical access, clear -plastic fixed volume cylinders were fabricated and installed into the engine head in place of the standard piston/cylinder setup. The bore of cylinder block was simulated using plexi-glass cylinders. The diameter and stroke of the plexi-glass cylinders was identical to that of the original. Intake valves were replaced

with 2.5 cm tubes to prevent the flows crossing to the exhaust valves directly. The exhaust valves were operated by a cam driven by a DC electric motor. Photographs of the engine head and cylinder assembly are shown in Figure 3 and Figure 4.

#### **B. Plastic Catalytic Converter**

The converter housing was fabricated from clear plastic to provide optical access for the LDV measurements and for the flow visualization. The plastic was molded into two pieces so that the catalyst brick could be inserted with ease. Figure 5 shows the two pieces of plastic model that were molded from the actual converter.

The two pieces were bolted together using 4 cm steel brackets around the edge. The steel brackets provides the necessary rigidity for the converter from the vibration from the engine. The putty used in the constructing of the converter into one piece, as a sealant. This prevents air leaking out of the converter. A picture of the assembled converter is Figure 6. Although the housing was fabricated of clear plastic for optical access, in the initial stage of the experiment many problems were found. Some natural properties of the plastic had significantly altered laser beam polarization when it passed

through the converter. This problem was later intensified when the laser beams passed through some areas of the converter containing sharp bends. Thus, when LDV measurements were taken along the major axes near the corners, the data rates were too low to obtain the needed information. To overcome these difficulties, windows were installed at the corner of the sharp bend areas.

#### C. Flow System

The flow system consists of a blower, laminar flow meter with differential pressure inclined manometer, and hoses to dispense the atomized di-octyl phthalate (DOP) which was used as laser light scatter for LDV measurements. The laminar flow meter was used to provide the means of measuring the flow rate by a connection to a differential pressure inclined manometer. For the proper air flow rate, a blower was throttled to control flow rate. A pipe (115 cm) was installed at the approach to the assembly to ensure that the approach flow to the element was unifrom. The relative length of the pipe is about ten times the diameter of the flow meter entrance.

# D. Electric Motor and Angle Encoder

The engine head was driven by a 3 hp DC electric motor that was connected to the cam shaft of the engine. A photograph of the 3hp DC motor is given in Figure 7. A generator pickup feedback controller was installed on the shaft of the electric motor to maintain uniform speed. Flow was examined based on the cam angle, which is detected by an angle encoder installed directly on the cam shaft. Figure 8 is a close up view of the angle encoder. This encoder generates two series of 1024 square pulses per revolution. These two series of pulses are offset a half pulse length from each other. The computer can count 4 times the number of pulses from these two series of pulses. For this study, 4096 pulses per revolution were used and this represents 0.088 degree of angular resolution.

# E. External Lubrication System

The engine head was lubricated in the same fashion as the actual engine, except that it used an external, closed system with an oil pump and a vacuum pump to control oil circulation. The oil pump supplies the oil to the engine head, and the vacuum pump draws the oil out of the head. It is also an

advantage to have negative pressure under the valve cover, as this reduces the chances that oil will travel down the valve stems. It is important to prevent the oil from going down the valve stems because the smearing oil could cause the refraction of the laser beam or cause microballoons to adhere to oily parts in the converter. A 10W-30 engine oil was supplied to the head through 0.635 mm tubing to the inlet port on the head face. After the lubrication of cams, the oil reservoir creates low pressure which draws oil and air from the engine head. The returned oil is then fed to the oil pump, which supplies filtered oil to the engine head. The schematic of the lubrication system is in Figure 9.

To accommodate all this equipment, a steel channel structure was built to include the engine head, intake and exhaust systems, electric motor control system, and engine oil supply system. The base measurements for the steel channel structure are 120 cm by 120 cm and the height is 225 cm. This steel structure was aligned to the LDV optical table for the catalytic converter to stand vertically. To prevent the vibration from the engine operation to the LDV optical table, rubber isolators were located under the 4 adjustable legs of the structure base.

# 2.2 High Speed Flow Visualization

The flow visualization technique has been facilitated through the use of a specially designed particle mixer. This device is designed so that it completely mixes the seed before entering the test area. Before the development of the mixer, particles were directed into the flow in small amounts through the intake port. With the new mixing device, particles can be completely mixed and stored in a large reservoir for continuous use during testing. This device is different from conventional particle seeders in which the entire mixture of fluid and seeding particles is stored in a chamber prior to entering the test section. A schematic of the mixer is in Figure 10.

# A. Seeding Particles for Flow Visualization

The seeding particles for flow visualization are phenolic microballoon particles supplied by Union Carbide and designated as BJO-0930 (density of 0.23 g/cm<sup>3</sup>). In earlier study, conducted by Schock et.al [6] it was discovered that these particles showed significant improvement in visual contrast over other seeding materials such as titanium dioxide or aluminum particles. This

improved light seeding particles for flow scattering ability provided more detail which allowed for a greater understanding of the major flow features.

The microballoons must be dried before entering the test area to prevent agglomeration. In the seeder, the mixing of the microballoons takes place in a 60-liter cylindrical enclosure. There are two mechanisms that are used to mix the particles once they are dried and placed onto the wire screen in the container. The first is a fan with a 3000 rpm motor that serves to agitate the microballoons and keep them swirling in the container. The fan is located just below the center of the container, therefore, any particles not entrained in the swirling motion of the fan will fall to a wire screen mesh located about 5 inches below the fan. The screen is a 40 x 40 lines per inch mesh, and the wire diameter is 0.01 inch. This mesh prevents clumps of microballoons from falling to the base of the container where the air inlet is located. Just above the mesh sits a two arm mixer driven by a 28 rpm gear reduction motor which serves to move and lift any microballoons that settle on the wire screen into the air stream of the fan. Once the inlet air is flowing through the screen, the microballoons are lifted off and tend to hover just above the screen. The rotating arms of the mixer then force the hovering microballoons into the air stream of the fan.

The air inlet and outlet for the seeder is made of 4-inch PVC tubing. The direction of intake air flow is governed by a throttle valve. The air will bypass the microballoons and the cylindrical enclosure when the valve is in the down position. The path of the air flow for the valve in the shown position is Figure 11 (a). When the throttle valve is up, air is redirected into the cylindrical enclosure and entrains the microballoons. The entrained air containing the microballoons is then sent to the test area through the outlet of the seeder. The outlet was placed at the top of the mixing chamber in order to minimize the number of heavy microballoon clumps that enter into the air flow. These clumps would tend to hover or swirl in the lower portion of the chamber.

There are various methods to control the number of microballoons. The first method deals with the amount of microballoons placed in the seeder. An accurate representation of the flow field could be altered if there are too many microballoons are used. The other method used to control the density concerns the position of the throttle. In the Figure 11 (c), if the throttle is positioned in the middle of the inlet pipe, the mixture entering the test area will contain pure air and air mixed with microballoons. This mixture of air and microballoons occurs because air travels through both the seeder bypass

and the seeder itself. Either one of the above mentioned methods can be used to control particle saturation.

The first step in operating the seeder is to lead the microballoons onto the wire screen and seal the lid on the container. The throttle should be in the down position to start with so that only pure air is sent to the test area which completely bypasses the wire screen covered with microballoons. important to avoid the entrainment of microballoons through the seeder and into the test area before they are actually needed. The next step is to turn on the agitating fan to stir up the particles. After this step, the throttle of flow valve is opened and mixing rotor is turned on. This ensures that the mixer will push hovering microballoons into the swirling motion of the fan. Once everything is turned on and the test area is ready, the throttling valve is then opened to redirect the flow into the seeder. When this happens, air travels through the inlet, up through the bottom wire mesh, and into the container. The swirling motion entrains the microballoons, and they are pulled through the outlet and into the test area.

#### **B. HSFV Hardware**

The high speed flow visualization system consists of a 40 watt copper vapor laser (CVL), a high speed camera, a synchronization system, a particle generator and optics. The CVL Model 451 is a gas discharge device of 40watt average output power manufactured by Metallaser Technologies. It emits short pulses at 5000 pulses per second (pps) and a pulse energy of 8 mJ in the green and yellow regions of the visible spectrum, at wavelengths of 510 and 578 nm (2/3 power at 510.5 nm, 1/3 at 578.2 nm). The rate of the pulse can vary between 4000-6000pps. The pulse duration is approximately 30 ns and pulse jitter is 3 ns. The main components of the laser are a plasma tube, high voltage DC power supply and a pulsed discharge system (thyratron driver and thyratron). The thyratron driver is a high voltage, high repetition pulse generator which provides trigger pulses to the thyratron. The laser operator could use the internal 5 kHz oscillator or apply an external pulse trigger select.

The laser beam, which has a beam diameter of 5.08 cm and has a Gaussian power distribution, is directed toward the converter by a set of three circular mirrors. A square cylindrical lens and a cylindrical mirror were used

to focus the beam into a light sheet approximately 1.5-mm thick. These mirrors together provide high resolution angular control with coplanar-orthogonal adjustments. This laser light sheet provides enough exposure to the films used for the high speed flow visualization.

A 16 mm Nac E-10/EE high speed rotating prism camera with a fast f 2.5 optical system is used to take flow images on a Kodak film (7292 tungsten, 320 ASA, 2-stops push processed to 1600 ASA). The camera is equipped with a trigger pulse generator and optical pick-up to trigger the CVL laser at 5 kHz and synchronize the laser pulses with the film frame rate of 5000 frames per second (fps) .[8]

An electronic timing system was designed and built specifically to switch thytatron driver of the CVL from internal to external mode. In the external mode the pulse generator of the camera triggers the laser during the filming process. At the end of the film the timing control switches the laser back to the internal mode. Also, the synchronization system can be used to control the operation of external parameters for a preset number of crank angles. The schematic is shown in Figure 12.

## 2.3 Laser Doppler Velocimetery

## A. Seeding Particles for LDV

An important consideration in LDV measurements is the selection of seeding material. The scattering particles are the basic source of the Doppler signal, and their importance in the overall performance of an LDV system should not be underestimated. By increasing the particle diameter from several tenths of a micron to several microns, the signal factor increases from  $10^2$  to  $10^4$ .

The particles used for seeding must be small enough to follow the fluid and not cross more than one fringe at once. On the other hand, if the seed particle size is too big, the particle will have inertial effects which prohibit it from following the flow. The practical limit which determines the particle following a turbulent flow is,  $\tau / T \le 0.02$  where  $\tau$  is the relaxation time of the particle and T is the Lagrangian macro time scale of the turbulence.[8] The particle relaxation time is given by

$$t = \rho_p d_p^2 / 18\eta$$
 (1)

where  $\rho_p$  is the particle density,  $d_p$ , is the particle diameter, and  $\eta$  is the average gas viscosity. The Lagrangian macro-time scale is given by

$$T = \varepsilon / v^{2}$$
 (2)

where  $\varepsilon$  is the momentum eddy diffusivity and  $v'^2$  is the turbulence intensity. These quantities can be written in more convenient form such as

$$\varepsilon = \mu / \rho_{air}$$
 (3)

$$v'^2 = (2/3) \text{ K.E}$$
 (4)

where  $\mu$  is the turbulence viscosity and K.E. is the turbulence kinetic energy.

Initially, water was atomized and used as the scatter particles in the air flow. This proved ineffective, though, because the water evaporated too quickly, Next, a mixture of propylene glycol and water was used. This combination also proved ineffective so pure DOP (Di-Octyl Phthalate) was employed. The DOP was able to scatter enough light to take the measurement.

#### **B. LDV Hardware**

One of the most important facts in describing flow phenomena is to conduct quantitative analysis. LDV is one of the best ways of conducting quantitative flow analysis. Figure 13 shows a schematic of the LDV system used for this study. LDV was employed to measure the velocity profiles inside the converter The three-component LDV system is composed of a 4-Watt argon-ion laser, beam collimator, polarization rotators, beam splitter,

beam steering lens, focusing and receiving lenses, digital burst correlator, traverse mechanism, and a computer for data acquisition. In order to measure three-dimensional velocity, the system is composed of an upper, one-component system for the fiber optics, and a lower two-color, four beam system. The one component fiber optic system is shown in Figure 14. Figure 15 shows the two component four beam system. The multi-wavelength beam is separated into several, single-wavelength beams by a prism. Two wavelengths ( green, 488.0 nm and blue, 514.5 nm) are selected to measure the two component velocity on the lower system. For the upper component another wavelength (violet, 476.5 nm) was directed with the fiber optic system.

The LDV configuration used in this experiment requires the laser beams to be transmitted through a beam splitter and Bragg cell. The beam splitter separates the laser beam into two equal intensity beams that are then focused onto the measurement location. Two blue beams (488 nm) were used for the v-component while the two green beams (514.5 nm) were focused for w-component measurements. A pair of violet beams (476.5 nm) was transmitted through fiber optics to measure the u-component velocity. A beam spacing of 50 mm and focal lengths of 453 mm ( for green and blue)

and 350 mm (for violet beams) resulted in the half angle values of 5.206° and 6.681°.

The two pair of beams (green and blue) from the lower component were setup so that the beams could transmit horizontally along the traverse. The violet beam from the upper component is split by Colorburst system which performs the function of a beam splitter, and a polarization rotor also directs the beams into fibers. A single violet beam is directed to the Colorburst, where it outputs a pair of violet beams. The beam exits vertically through a fiberoptic probe where it is used to measure the velocity component perpendicular to x and y. Figure 16 shows the fiberoptic tube mounted perpendicularly to the converter.

The LDV measures fluid velocities by detecting the Doppler frequency shift of laser light that has been scattered by small particles (0.1 to 10 µm) flowing with the fluid. It is also important to select the particles that follow the fluid flow and have a large refractive index at the wavelength used for the measurement. To accomplish this, a Six-Jet Atomizer (TSI Model 9306)was used to atomize DOP for laser light scattering particles.

The atomized DOP joined the air stream just prior to the flow entrance into the intake manifold. A long, narrow leading tube was used to connect the atomized fluid with the air stream at the center of the air supply tube. The

scattered light is collected by a photomultiplier detector and converted into voltage signals. The velocity of the particles in the fluid is proportional to the Doppler frequency and can be determined by the relationship as

$$V = d_f / t_I = d_f * F.$$
 (1)

where

 $d_f$  = fringe spacing,

 $t_1$  = time taken for the particle to cross a pair of fringes,

F =Doppler shift frequency of the scattered light.

The relationship used to determine the velocity of the particles traveling with the fluid flow is shown in Equation (1). The fringe spacing,  $d_f$ , can be readily determined by

$$d_f = \lambda / (2 \sin \kappa) \dots (2)$$

where

 $\lambda$  = wavelength of the laser light,

 $\kappa$  = half angle between the beams.

The Doppler shift frequency, F, is measured in Hz and is equal to the number of fringe patterns a particle crosses in one second. A frequency shifter is used to measure flow reversals. The system works by having the

Bragg cell use the interaction of laser light and high frequency ultrasound in a transparent medium to shift the frequency. Three frequency shifters were employed, one for each color. The IFA 750 Digital Burst Correlator was used to measure the frequency of the burst signal. The three-channel correlator analyzes the Doppler signals so that three velocity components at the measured position can be calculated separately [7-11].

One of the greatest advantages of LDV as opposed to other flow measuring techniques such as pitot tubes and hot-wire anemometers is its characteristics of being non-intrusive. Unlike pitot tubes, LDV has no effect on the flow stream because there is no physical measuring device to restrict the flow. Also one can measure flow reversals with the LDV system.

# 2.4 Computer Animation

LDV measurement is a technique to measure ensemble-averaged velocity vectors at a measurement volume, while flow visualization shows the cycle-resolved velocities in a plane. Since LDV is a point measurement technique, it does not show the flow patterns directly. It is useful if a set of the LDV measurement data can be animated in time. This animated LDV result can be easily compared with the flow visualization results. PV-WAVE

visualization software was employed to animate LDV measurement data on a SUN workstation. The software creates 40 or 50 images and runs them continuously.

#### **CHAPTER 3**

#### EXPERIMENTAL PROCEDURE

# 3.1 Coordinate System

An explanation of the terminology and coordinate system used for this study is now given. Cartesian coordinates were employed for the flow measurements and analysis. Figure 17 (a) shows the coordinate system in the catalytic converter. Figure 17 (b) is the view from the top. The streamwise air flow direction was chosen as positive z direction, and the plane perpendicular to the z-axis was defined as the x-y plane. The x-axis is perpendicular to the engine crankshaft, while the y-axis is parallel to the engine length. The positive x-value represents the direction away from the engine and the positive y-value stands for the direction toward the first cylinder (see Figure 1). The origin of the x-y coordinate system is at the center of the measured plane.

# 3.2 Experimental Sequence

The test system was initiated by a specific sequence of steps. First, the vacuum pump was turned on to drain residual oil in the head. The oil pump was started to supply filtered engine oil to the engine head.

Oil flow was checked by observing the tygon tubing for oil flow and by monitoring the vacuum gauge. The DC motor was then activated and set to the appropriate engine speed. The blower system was turned on and allowed to run for 10 to 20 minutes before throttling to the correct flow rate in order to provide steady flow to the system.

# 3.3 Quantitative Measurement

Although, the flow visualization technique can determine the bulk feature, the differences of these features are often subtle and cannot be described in a quantitative way. Therefore quantitative analysis is important to understand the flow characteristics in a highly fluctuating turbulent flow like the one in the catalytic converter. To measure the local velocities and fluctuations, a three-component LDV system was employed. The three velocity component are crucial to understanding the nature of the turbulent

flow inside the catalytic converter which cannot be determined by measurements of individual components.

One of the important characteristics of turbulent flow is that of its irregularity or randomness. Statistical methods are used to define such flow field. The quantities that characterize turbulence are usually the mean velocity and the fluctuation velocity about the mean, and length and time scale. The local instantaneous velocity can be defined by

$$U(t) = \overline{U} + u'(t) \tag{1}$$

Here, the mean velocity is the time average of U(t)

$$\overline{U} = \lim_{\tau \to \infty} \frac{1}{\tau} \int_{t_0}^{(t_0 + \tau)} U(t) dt$$
 (2)

The turbulent portion of the velocity is u'(t). For a steady flow, the mean stands for the simple time averaged value. In the converter, the flow pattern changes during the engine cycle. The mean value can vary significantly from one engine cycle to the next. Instantaneous velocity can be written as a function of cam angle  $\theta$  and cycle number instead of a function of time.

$$U(\theta, i) = \overline{U}(\theta, i) + u'(\theta, i)$$
(3)

The ensemble averaged velocity  $U_{ea}(\theta)$  over Nc cycles can be defined as

$$\overline{U}_{ea}(\theta) = \frac{1}{Nc} \sum_{i=1}^{Nc} U(\theta, i)$$
(4)

where the Nc is the number of cycles for which data is available. The ensemble average velocity is only a function of cam angle since the cyclic variation has been averaged out. The difference between the mean velocity in a particular cycle and the ensemble-averaged mean velocity over many cycles is defined as the cycle-by cycle variation in mean velocity

$$\hat{U}(\theta,i) = \overline{U}(\theta,i) - \overline{U}_{ea}(\theta)$$
 (5)

Thus the instantaneous velocity can be split into three components

$$U(\theta, i) = \overline{U}_{ea}(\theta) + \hat{U}(\theta, i) + u'(\theta, i)$$
(6)

This is the most desirable equation to be used for the measuring velocity in the converter. By maintaining constant engine speed the variation from one cycle to another  $(U(\theta, t))$ .

The ensemble averaged fluctuation  $u'_{ea}(\theta)$  is given by

$$u'_{ea}(\theta) = \frac{1}{Nc} \sum_{i=1}^{Nc} u'(\theta, i)$$
 (7)

It includes all fluctuations about the ensemble averaged mean velocity.[12] Based upon equation(6) and (7), ensemble averaged mean velocity and mean fluctuation were calculated.

The LDV measurements were conducted in two planes: the inlet plane and the midsection plane. The inlet plane is located 2.5 cm in front of the first catalyst brick in the inlet plenum, and the midsection plane is the center plane between the catalyst bricks (see Figure 17 (a)). Ensemble-averaged velocity vectors [4,5] were measured by LDV for a total of 300 points for two different flow rates. LDV measurements were conducted along two major axes and two minor axes in each plane. The two major axes' locations are x = 12.5 mm and -16.5 mm, while y = +30 and -30 mm were chosen for two minor axes (see Figure 5). Three components of velocity were measured at each point along the major axes. Because of problems with laser beam access due to the seam between the two halves of the converter, two components of velocity vectors (u and w) were measured along the minor axes. Measurements were taken every 5 mm along the major axes and every 3 mm along the minor axes.

#### 3.4 Flow Visualization

The CVL is used as a light source for the high speed flow visualization process. Once the CVL beam is on, the optics are adjusted to form a light sheet through the area of interest. When a laser beam with a power of 25-30 watts is achieved, a test run of the camera is performed to verify that the shutter is synchronized with the laser pulses at 5 kHz. The film is then loaded, and the camera positioned and focused on the light sheet in the cylinder, which was filled with incense smoke to scatter light for focusing. The seed generator is loaded, sealed, and connected to the intake manifold. The exhaust fan and lubrication system are turned on while the laboratory lights are turned off to reduce unwanted light intensity to the camera. The rig is then motored at the desired speed. The seeding particles are phenolic microballoons with an average diameter of 40. The microballoons are introduced into the converter through the intake manifold, pass into the fixed volume cylinder, and finally to the exhaust manifold. The flow in the system is very complicated, and high-frequency periodic flows are present. It is necessary to take the images at high speed to obtain a satisfactory level of clarity of the unstable flow features. For this visualization, the camera was

run at a film speed of 5000 fps. At this speed 120 m of movie film is exposed in approximately in 3 seconds. Four flow-visualization films were taken at planes in the inlet plenum of the converter. Flow was examined at two different engine speeds (2000 and 4000 rpm) with two different flow rates (120 and 205 scmh).

There are four planes chosen for flow visualization films. Figure 17 shows the four planes in which the flow visualization films were taken. The first character of the planes (H or L) stands for the high or low flow rates. The second character (1 or 2) means a plane parallel to the major (1) or minor (2) axis. The H1 and L1 planes are defined as planes parallel to the major axis of the catalyst brick and the H2 and L2 planes are parallel to the brick's minor axis with high and low flow rate, respectively.

Planes H1 and L1 are identical planes in different operating conditions. To take films for these planes, a laser sheet was provided from the 4th cylinder side. The back face of the converter was painted black to prevent interference from reflections. The camera was positioned at 90 degrees to the laser sheet.

Planes H2 and L2 were located slightly apart. The H2 plane is offset approximately 1.5 cm from the center of the converter to observe the effects

of the oxygen sensor on the flow in the inlet of the converter. Plane L2 was located at the center of the converter to observe the flow on the minor axis. Flow visualizations at 1000 and 2000 rpm were found to be similar. Due to the flow similarity it was valuable to examine the flow around the oxygen sensor to check the viability of the sensor location.

#### **CHAPTER 4**

#### **RESULTS AND DISCUSSION**

## 4.1 Exhaust Manifold Consideration

Interpreting the results from LDV measurement and flow visualization in a catalytic converter under normal engine operating conditions requires evaluating a large amount of data. Even though LDV measurements are different from the flow visualization results, it is easier to understand the flow characteristics when the results are compared in the same manner. It is much easier to understand when the flow visualization films have been seen.

Before examining the flow patterns, it is important to understand the exhaust manifold configuration. Four exhaust paths from the four separate cylinders are merged into two passages at the end of the exhaust manifold. Exhaust paths from cylinder 1 and cylinder 4 are combined and go through an inside partition (near the engine), while exhaust paths from cylinders 2 and 3 go through an outer partition (away from the engine). It is also necessary to discuss engine firing order because it relates to the exhaust valve opening and

closing orders. Figure 19 shows the typical valve timing for a four-cylinder, four-stroke engine with a 1-3-4-2 firing order.

## **4.2 Flow Visualization Results**

Figure 20 shows the sketches of flow patterns from the high speed flow visualization films. However, the arrows in the sketches do not represent the velocity magnitude. Figures 20 (a) and 20 (b) are the side view from the cylinder 1 side (H2 and L2 in Figure 17), while Figures 20 (c) and 20 (d) are the front view from the opposite side of the engine location (H1 and L1 in Figure 17).

Figure 20 (a) is a flow pattern produced by the exhaust from cylinder 2 or 3. Figure 20 (b) shows that from cylinder 1 or 4. The downward pulse on one side and the backflow on the other side in Figure 20 (a) are stronger than those in Figure 20 (b). This phenomenon can be explained by the configuration of the exhaust manifold. The exhaust passages in the manifold from the cylinder 1 and 4 are connected at the converter flange with a 90° bend, while the passages from the cylinder 2 and 3 have a straight connection. So, the exhaust flow from the cylinder 2 or 3 is faster and uses a smaller area of the converter than the flow from cylinder 1 or 4.

Figure 20 (c) represents the flow pattern of exhaust from cylinder 3 or 4, while Figure 20 (d) shows that from cylinder 1 or 2. The exhaust manifold used for this study is slightly asymmetrical about its center. Even with this asymmetry of exhaust passages, the flow patterns are similar to each other (Figures 20 (c) and 20 (d)). The effect of the shape of the exhaust manifold can be observed in the direction of the flows in the converter. The exhaust from cylinders 1 and 2 travels from the left to the right, creating a pulse in the converter to the right. The exhaust from cylinders 3 and 4 travels from right to left, creating a pulse on the left side of the converter. In both cases regions of recirculation form in the far corners of the converter. For both cases, the flow speed from cylinder 2 or 3 is faster than from cylinder 1 or 4. The exhaust from the cylinder 2 or 3 flows mainly through the middle portion of the converter, and the exhaust from cylinder 1 or 4 directed to the opposite side of the manifold passage.

#### **4.3 LDV Results**

Figure 21 contains pictures of the catalytic converter used for this study and the wire mesh model used in the animation of the LDV data. Figures 21 (a) and 21 (c) are the front view of converter (from the exhaust side of the

engine) and Figures 20 (b) and 20 (d) are the side view from the cylinder 1 side. In order to simplify the presentation of the results, the wire frame was removed, and the two planes of interest were printed together. Figures 24 to 25 show the animated velocity vectors at specific cam angles. The pictures on the left side is the viewpoint from the exhaust side of the engine, the same as Figure 20 (c). The pictures on the right is observing the from the side of cylinder 1. This view point is same as the one shown in Figure 20 (d). For the pictures on the left, cylinder 1 is to the left and cylinder 4 is to the right. The main flow direction (positive z-direction) is toward the bottom of the converter, where the exhaust gases exit. The cam angle for the velocity profile is provided for each set of pictures.

Eight lines of vectors are drawn for each angle: four parallel to the major axis (left to right in the figures) and four parallel to the minor axis (top to bottom in the figures). The top of the catalytic converter is rotated around the y-axis counter clock wise (see Figure 17 (b)) to ease the view of the four major and minor axes. The upper four pair of vectors are the measurement from the inlet portion while the lower four pair are the midsection. For the major axes, the upper row of vectors are at x = -16.5 mm, while the bottom row is at x = 12.5 mm. In reference with the view point of Figure 20 (c), the

column of vectors for the minor section is located on the left side at y = 30 mm, while the right side column is at y = -30 mm.

Regular vector arrowheads from PV-WAVE did not show up well in printouts of the three-dimensional vector fields. Asterisks proportional to the vector magnitude were placed at the heads of the vectors in place of the arrowheads. Since the rows of vectors parallel to the major axis are three-dimensional, their 2-D lengths may not be proportional to their magnitudes. A scale is provided to estimate the magnitudes.

Figure 24 is the results from the low flow rate set-up (engine speed of 1000 rpm and flow rate of 120 scmh). Figure 25 is the high flow rate set-up (2000 rpm and 205 scmh).

For the low flow rate (Figure 24), the results show that the velocity distributions are quite complicated and the flows are periodic with a high frequency. The figures show that the exhaust manifold configuration has an effect on the flow direction in the inlet plenum. In early cam angles, the exhaust gas flows to the right side. This indicates that the air from cylinder 1 is still affecting the flow. At a cam angle of 43.4 degrees, most of the exhaust flows through the left front section of the converter, as the exhaust from cylinder 3 reaches the converter plenum. At the right side and back of the

plenum at this angle, a flow reversal was observed. The left side flow stays developed until the exhaust from cylinder 4 arrives. At cam angle 101.3, this flow from cylinder 4 becomes the main flow, and a strong flow on the back right side is developed. Around a cam angle of 230 one can observe a strong flow in the front of the converter from cylinder 2. This flow pattern is a mirror image of the flow at 43 degrees. At a cam angle of 307 the flow from cylinder 1 becomes the main stream in the back of the converter. The exhaust from cylinders 2 and 3 mainly flows through the front section (positive x), and the exhaust from cylinders 1 and 4 through the back section (negative x). The exhausts from cylinders 1 and 2 flow to the right side of the plenum, while those from 3 and 4 flow to the left side. This shows that the flow in the inlet plenum is affected mostly by the configuration of the exhaust manifold.

The periodic phenomenon in the midsection appears later in the engine cycle than in the inlet plenum. At around 60 degrees of cam angle, flow velocity from cylinder 3 becomes high in the front section. About 90 degrees later (159.2 degrees) one can see a strong flow in back of the converter. At cam angles of 250 and 350 degrees, flow patterns which are mirror images of those at 60 and 159.2 degrees, respectively, are observed. The two major differences between the flows in the inlet plenum and the midsection are the

direction and magnitude of the velocity vectors. In the inlet region, peak velocities for the two flow rates were around 30 m/s and 23 m/s; while between the two bricks, peak velocities were around 14 m/s and 6 m/s. Also, in the inlet plenum the difference between the maximum and minimum velocities is much bigger than in midsection, because flow reversals are present in the inlet region but absent in the midsection.

For the case of 2000 rpm and 205 scmh, general flow patterns were similar to those under 1000 rpm and 120 scmh configuration (see Figure 24). For both cases, the flow from cylinders 2 or 3 is directly injected to the converter, with most of the exhaust gas flowing through the front section of the converter. Exhaust from cylinder 1 or 4 are injected into the far side of the converter.

The flow field inside the converter is highly complex. Due to its complexity, the velocity profiles are not easy to understand. To aid in the understanding, separate points from the inlet plenum were plotted with the velocity magnitude corresponding to the engine crank angle. As with the PV-WAVE velocity profile, P1,P2,P3 is located at the lower horizontal line. P4, P5, P6 is located at the top horizontal line. Figure 22 is the location of the six points that were picked. As mentioned earlier, the main flow direction is the

positive w- velocity. Figure 23 is the graph of the velocity magnitudes with respect to the crank angle.

In early cam angle stages, gas exhaust is to the right side of the converter in the page. It could be seen from the graphs at x = -16.5 mm, the + w velocity is a weak flow, the flow at x = 12.5 mm has the dominance. This is an indication that cylinder 1 is still dominating the flow.

At a cam angle of 43 degrees, the exhaust from cylinder 3 reaches the converter plenum. Most of the exhaust flows through the left front section of the converter. At this stage, P1 at x=12.5 mm starts to show a rise in the flow magnitude as well as the upper region. However, the flow velocity starts to drop (back flow starts to form) starting at 43 degrees for P3. Around a cam angle of 230 one can observe strong flow in the front(x=12. 5) of the converter from cylinder 2. Because the flow magnitude is relatively greater at the lower right portion, the velocity of P1 becomes the greatest. In looking at the graphs, flow fluctuates heavily at the lower line (x=12.5 mm) than the upper line (x=-16.5). It can be observed that from the velocity profile, the flow is concentrated more at the front portion of the converter.

Regions of circulation in the inlet plenum were observed from the flow visualization films. The flow visualization films showed the same results as

LDV measurements. On the minor plane films (H2 and L2), a weak circulation was observed just before the flow changed from the back section to the front of the exhaust manifold. Strong separations in the major planes (H1 and L1) occur at the entrance region of the converter. When the exhaust from cylinder 2 or 3 starts to flow, weak circulation regions have been observed on both sides of the converter. For the flows from cylinders 1 and 4, a strong circulation on the opposite side and a weak circulation on the same side of the exhaust manifold passage tube were created.

The most used area of the first catalyst brick is the middle front region. The back section of the middle region is partially exposed to the exhaust gas when the flows from cylinder 3 or 4 are fully developed. The magnitudes of the velocity vectors at the major axes were much smaller at x=-16.5 mm than at x=12.5 mm., and more recirculation is present in the back (i.e. x=-16.5 mm) than in the front (i.e. x=12.5 mm). Both ends of the major axes experienced circulation for large amounts of time. This indicated underuse of the end regions of the catalyst and overuse of the central region, which will reduce the life time of the catalytic converter in actual engine operation. The plane between the two bricks has a more uniform flow distribution overall, but for the high flow rate, pulses in the flow were observed. The front section

of the converter had higher velocities, on average, than the back. The middle region of the two major axes also had much higher peak velocities than the end points. The second brick had a fairly uniform flow distribution for the low flow rate.

Flow around the oxygen sensor was studied by careful examination of the film for the plane H2. This showed that the oxygen sensor had little effect on the flow. It also showed that the oxygen sensor does not monitor the exhaust gases for a whole cycle. The trajectory of the exhaust from cylinders 2 and 3 was such that the majority of the flow did not touch the oxygen sensor directly. Also, the gas from cylinder 4 flows toward the side opposite the oxygen sensor without reacting with the oxygen sensor. The location of the oxygen sensor seems to be too close to the exit of the exhaust manifold to insure constant monitoring of the exhaust gases.

#### CHAPTER 5

## CONCLUSIONS AND RECOMMENDATION

After careful examination of the experimental results, the following conclusions have been reached:

- 1. The flow visualization techinque developed offers an effective method of examining the effect of the highly complex flow inside the catalytic converter. The combination of flow visualization and LDV measurements makes it possible to interpret the internal flow.
- 2. Dynamic flow characteristics were different from those under steady flow conditions in the catalytic converter. Therefore, to design the best converter possible, it is necessary to study flow characteristics in the catalytic converter under normal engine operating conditions.
- 3. Redesign of the angle, diameter and length of the entrance region is needed to prevent the separation and circulation present in the converter, thereby increasing the amount of active surface area used.

- 4. To reduce the periodic effect on the flow pattern, the size and configuration of the exhaust manifold must be reconsidered. A new design should direct the flow from each cylinder straight into the neck of the converter assembly as much as possible.
- 5. With the current exhaust system, the oxygen sensor is not continually exposed to direct exhaust emissions from each cylinder. The position of the sensor should be changed or the flow should be altered as recommended above.
- 6. The oxygen sensor generates a small wake, but does not create a significant disruption of the flow.
- 7. Velocities are greatly reduced and are more uniform after the first catalyst brick. The space between the catalyst bricks of present design seems to work properly.

8 The catalytic converter used for this study is relatively well designed for uniform flow distribution, and hence to have a long life.

## **REFERENCES**

- 1. Wendland, D.W., and Matthes, W.R., "Visualization of Automotive Catalytic Converter Internal Flows," SAE Paper No. 861554, 1986.
- 2. Wendland, D.W., Sorrell, P.L. and Dreucher, J.E., "Sources of Monolith Catalytic Converter Pressure Loss," SAE Paper No. 912372, 1991.
- Wendland, D.W., Matthes, W.R., and Sorrell, P.L. "Effect of Header Truncation on Monolith Converter Emission-Control Performance," SAE Paper No. 922340, 1992.
- 4. Lemme, C.C., and Givens, W.E., "Flow through Catalytic Converters An Analytic and Experimental Treatment," SAE Paper No. 740243, Feb 1974
- 5. Howitt J.S., and Sekella, T.C., "Flow Effects in a Monolithic Catalytic Converters," SAE Paper No 740244, Feb 1974
- 6 Schock, H.J., Hamady, F.J., Defilippis, M.S., Stuecken, T., and LaPointe, L.A., "High frame Rate Flow Visualization and LDV measurement in a Steady Flow Cylinder Head Assembly," SAE Paper No 910473, Feb 1991
- 7. Lee, K., Yoo, S.-C., Stuecken, T., McCarrick, D., and Schock, H.J., "An Experimental Study of In-Cylinder Air Flow in a 3.5L Four-Valve SI

- Engine by High Speed Flow Visualization and Two-Component LDV Measurement," SAE Paper No. 930478, 1993
- 8. Regan, C.A., Chun, K.S. and Schock, H.J., "Engine Flow Visualization
  Using Copper Vapor Laser," Proceedings of SPIE, Vol. 737, pp. 17-27,
  1987.
- Lee, K., Yoo, S.-C., Weber, M., and Schock, H.J., "Flow Characterization through a Catalytic Converter Using Laser Doppler Velocimetry," Technical Report MSUERL-93-2, Submitted to Ford Motor Co., 1993.
- 10 Instruction Manual for Digital Burst Correlator, TSI Inc., April, 1991.
- 11 .Adrian, R., "High Speed Correlation Techniques," TSI Quarterly, Vol VIII, Issue 2, April-June, 1982.
- 12 Heywood, J.B., "Internal Combustion Fundamentals," McGraw-Hill,
  New York, 1988

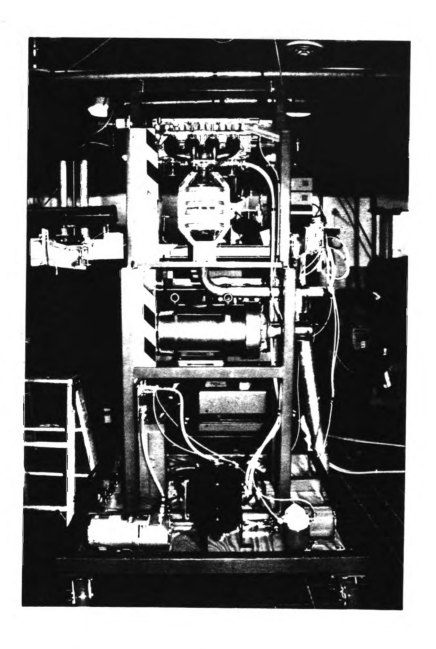


Figure 1. Photograph of the test bench

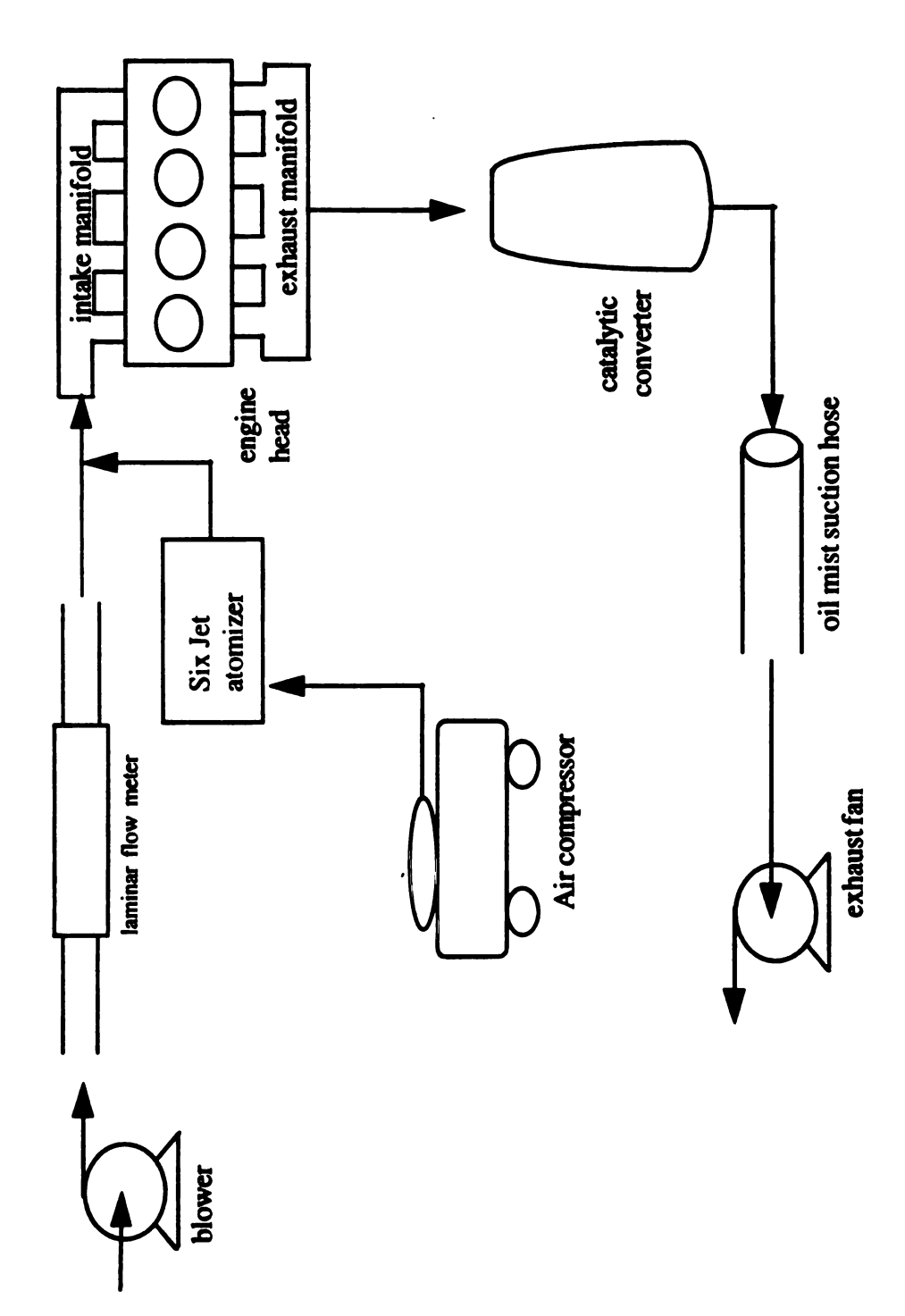


Figure 2. Schematic of the catalytic converter system

49



Figure 3. Photograph of the clear plastic cylinder assembly

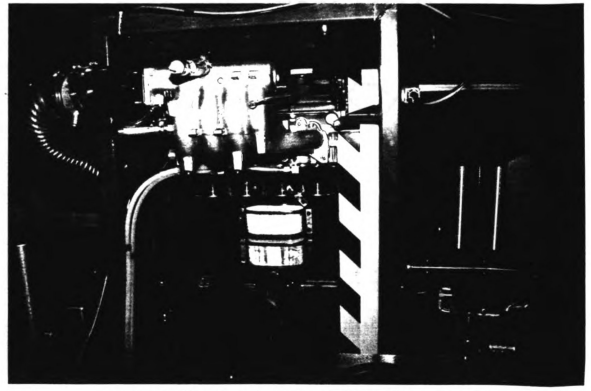


Figure 4. Plastic cylinder assembly on the test stand



Figure 5. Photograph of the two piece converter

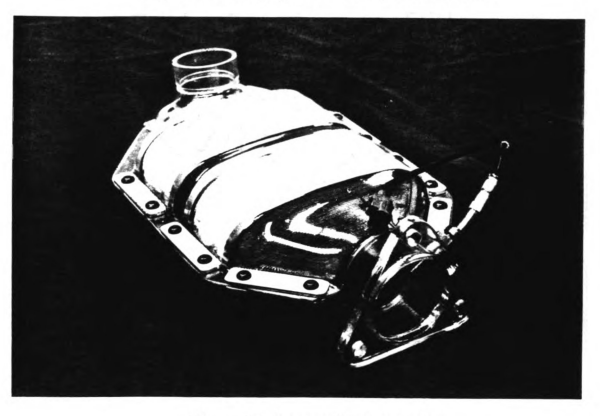


Figure 6. The assembled converter

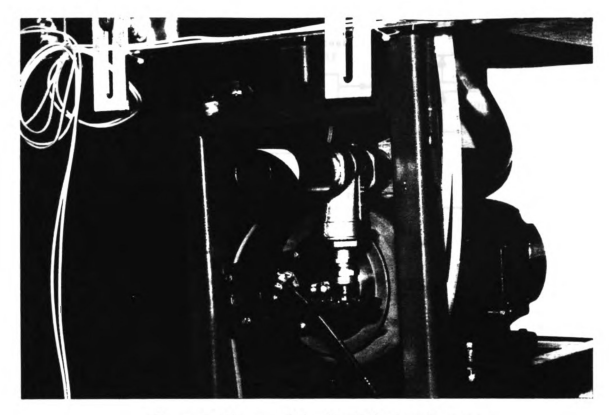


Figure 7. Picture of the 3hp DC electric motor

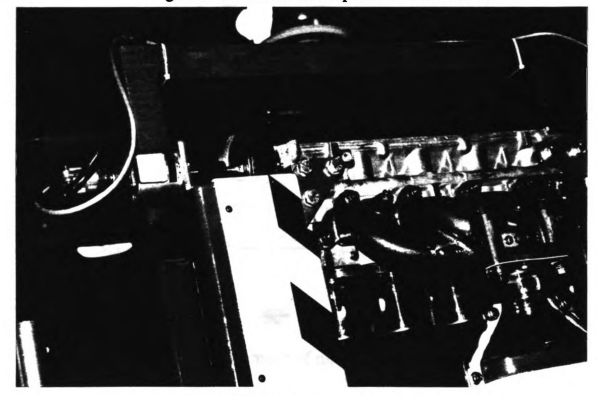


Figure 8. Picture of the angle encoder

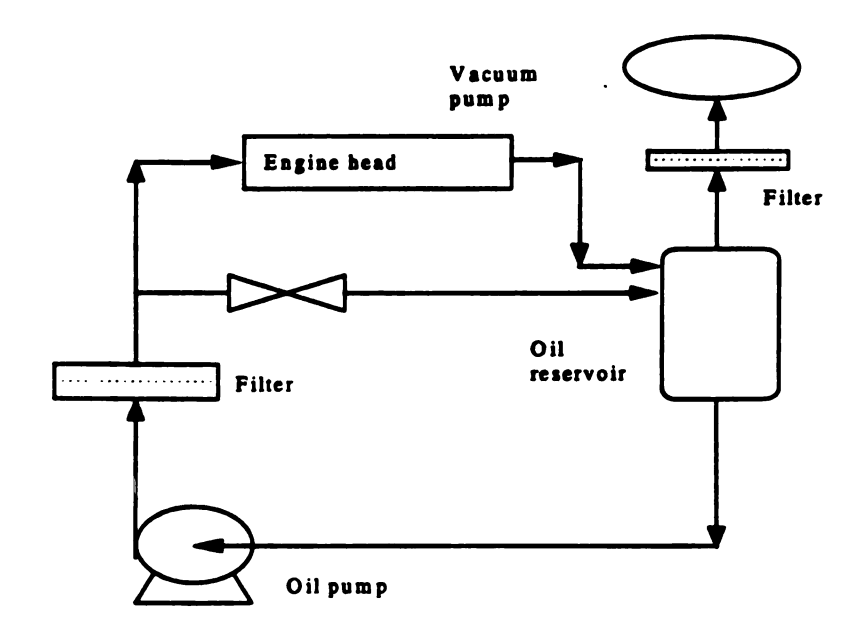


Figure 9. Schematic of external oil supply system

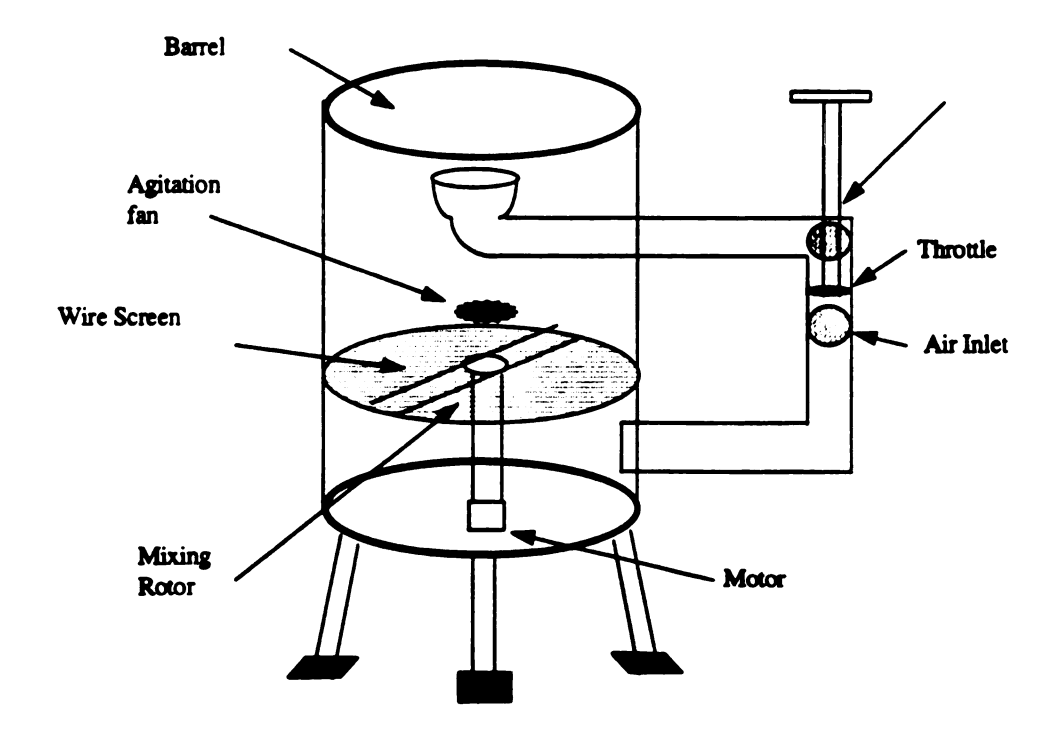


Figure 10. Schematic of microballoon seeder

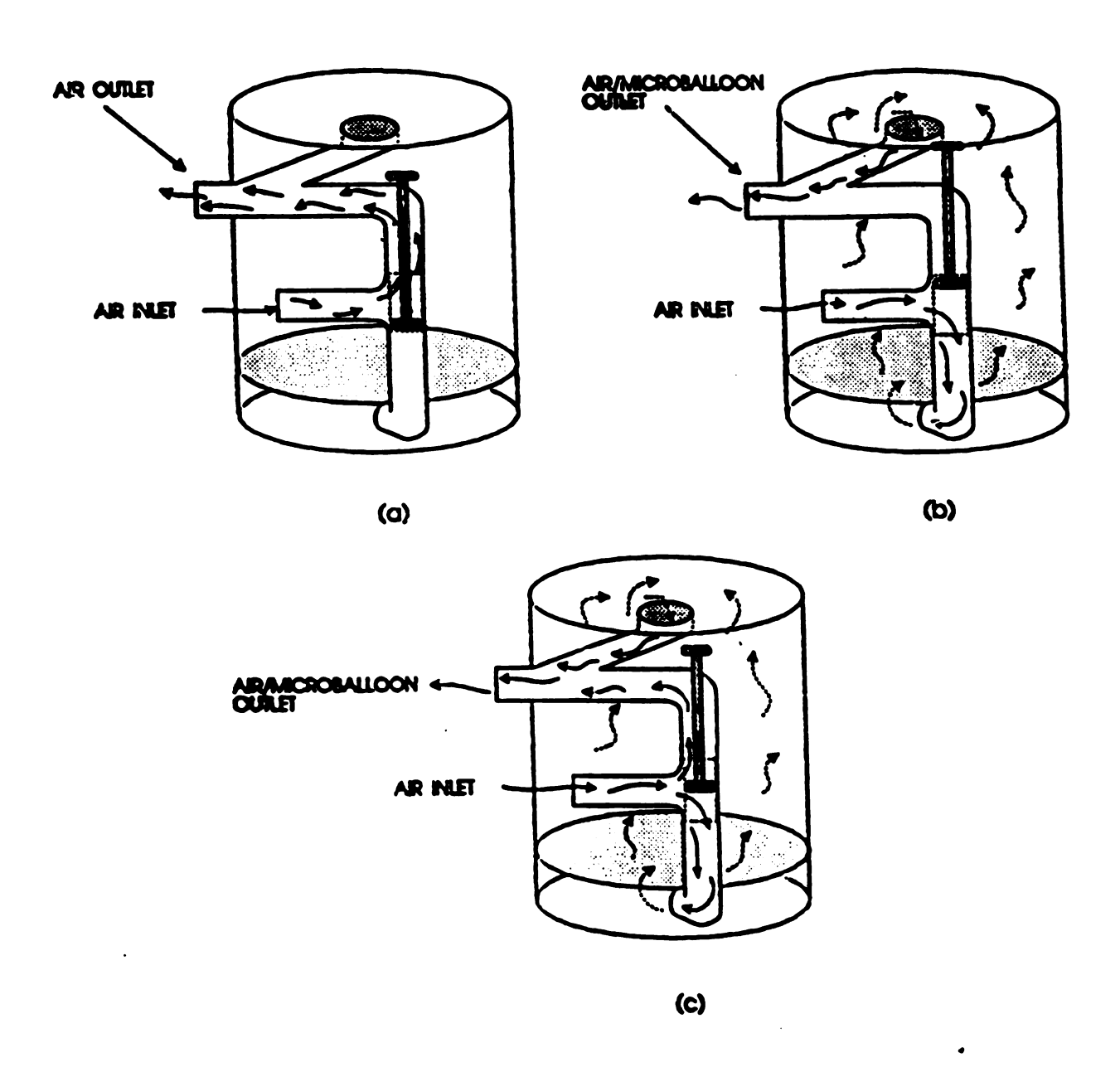


Figure 11. Microballoon seeder illustrating a) bypass flow, b)flow through the container and c) throttled flow containing air and seed.

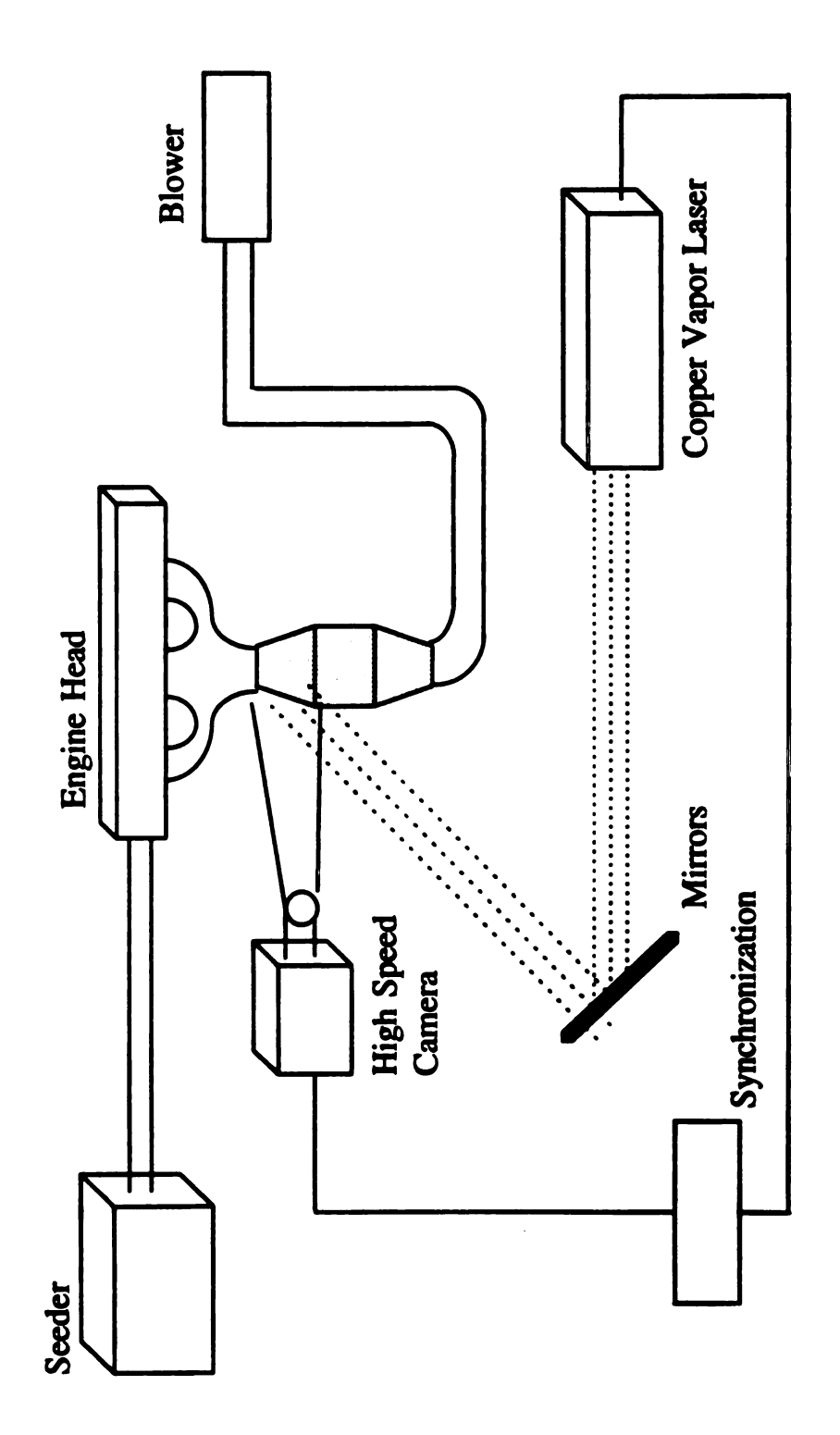
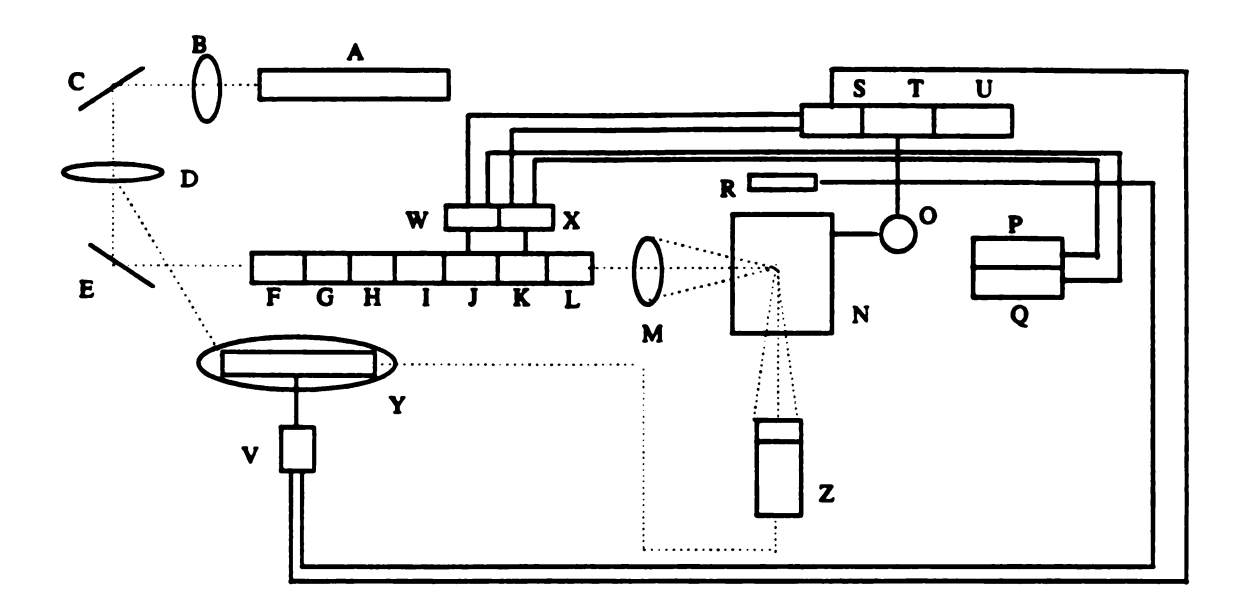


Figure 12. Schematic of the flow visualization setup



- A) Argon -Ion Laser
- B) Beam Collimator
- C) Steering Mirror
- D) Prism
- E) Steering Mirror
- F) Beam Splitter 488.0 nm
- G) Beam Splitter 514.5 nm
- H) Polarizer 488.0 nm
- I) Polarizer 514.5 nm
- J) Bragg Cell 488.0 nm
- K) Bragg Cell 514.5 nm
- L) Beam Stop
- M) Focusing Lens

Figure 13 LDV system.

- N) Catalytic Converter
- O) Shaft Encoder
- P) Receiving Optics 514.5 nm
- Q) Receiving Optics 488.0 nm
- R) Receiving Optics 476.5 nm
- S) IFA 750 Signal Processor
- T) Rotating Machinery Resolver
- U) Master Interface Unit
- V) Frequency Shifter 476.5 nm
- W) Frequency Shifter 488.0 nm
- X) Frequency Shifter 514.5 nm
- Y) Colorburst
- Z) Fiberoptic Probe

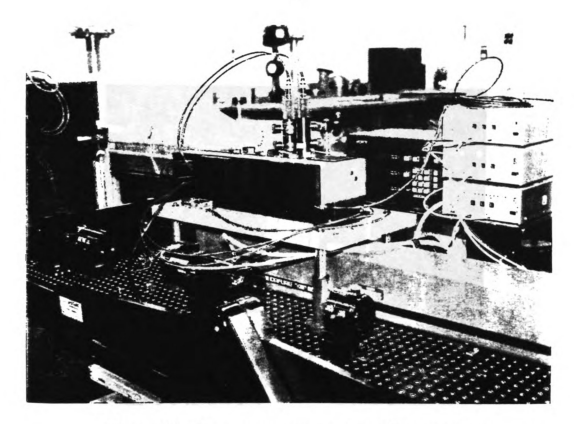


Figure 14. Upper one component two beam system

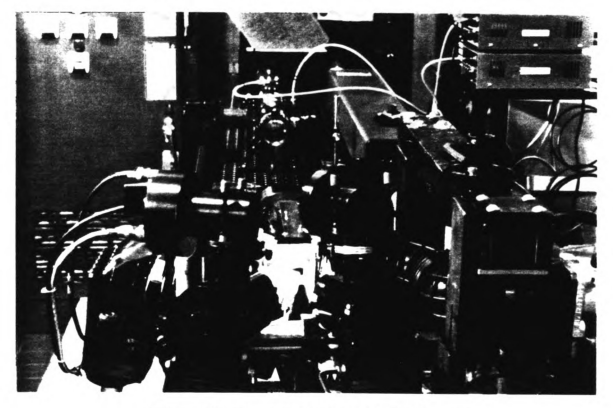


Figure 15. Lower two component 4 beam system

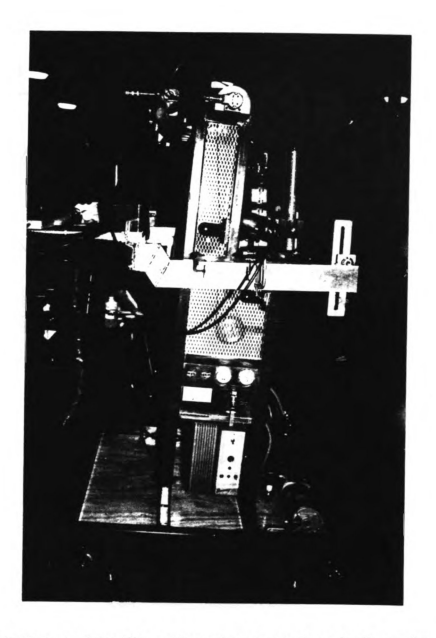


Figure 16. Picture of the fiberoptic probe mounted vertically on the converter.

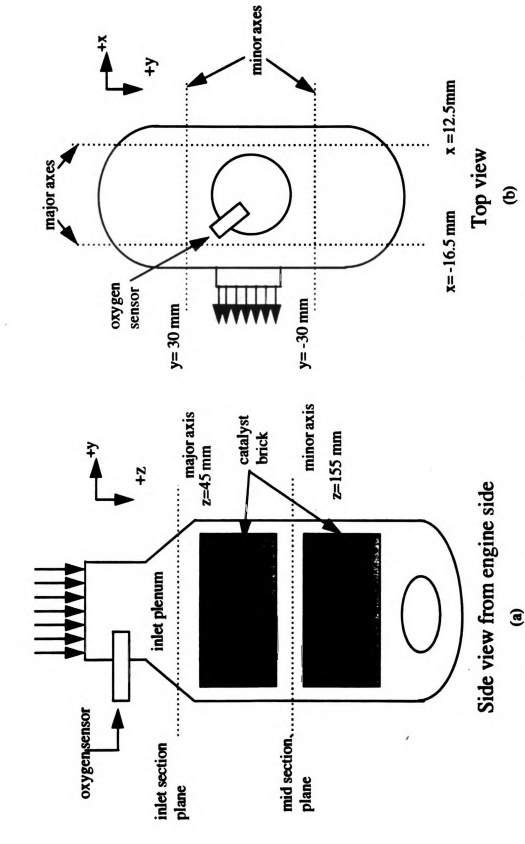
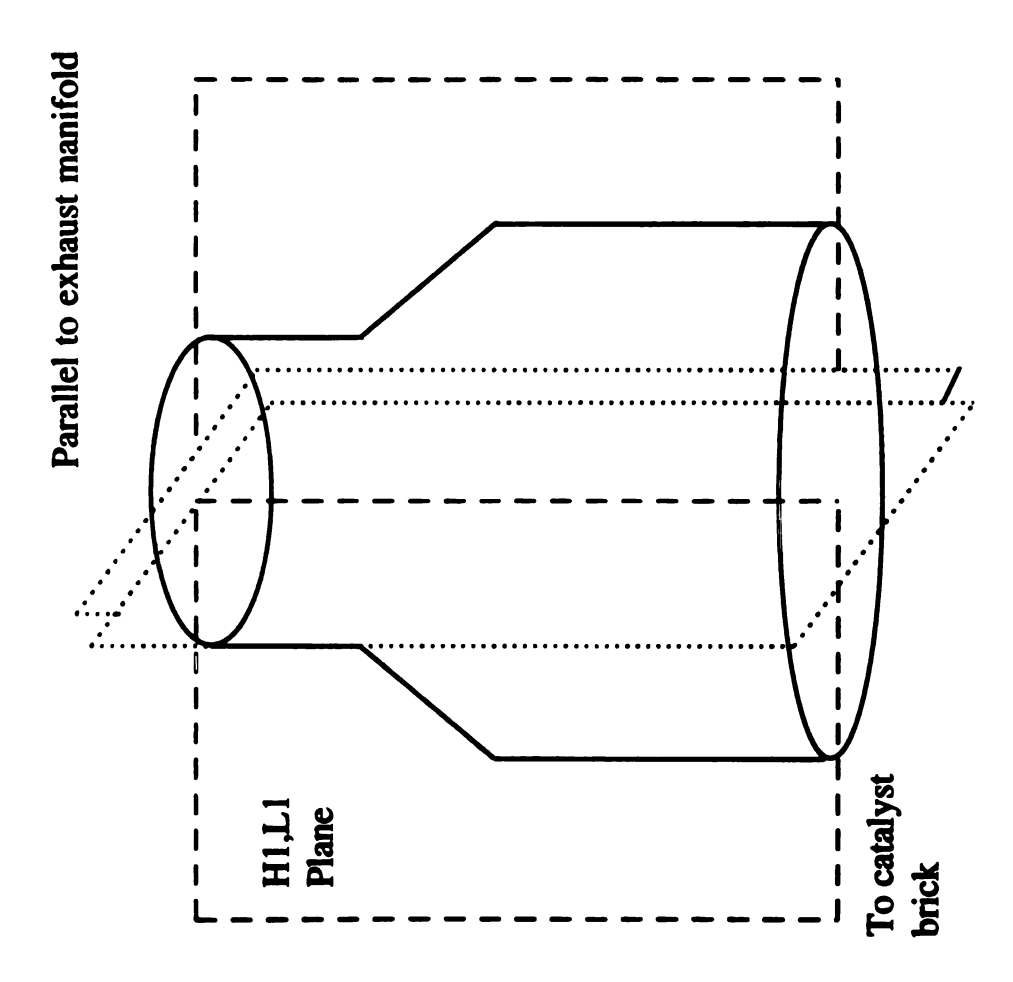


Figure 17. Coordinate System and Coordinate Axes Description for Catalytic Converter



to the major axis and H2 and L2 are the planes parallel to minor axis Figure 18. Flow visualization planes. H1 and L1 are the planes parallel

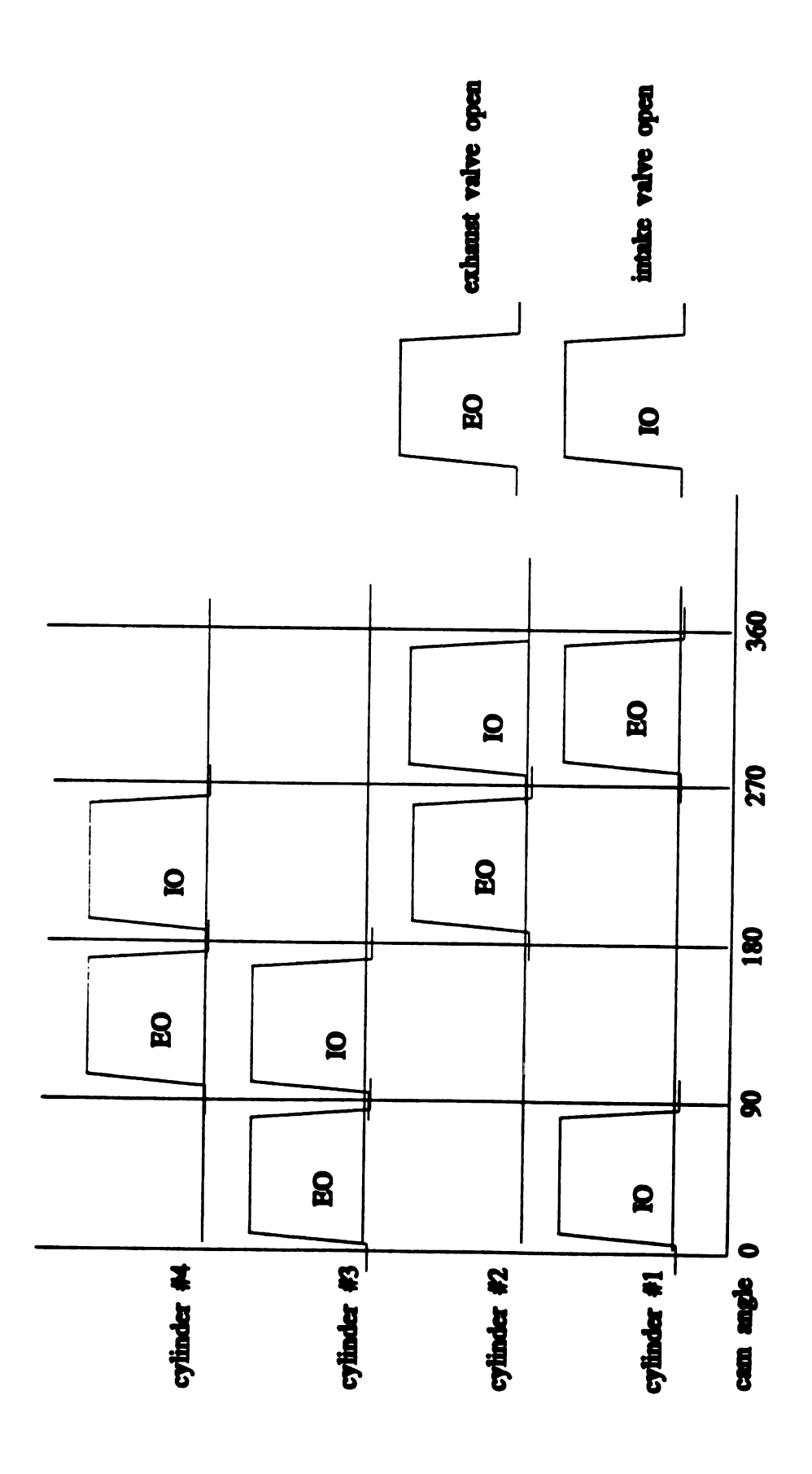
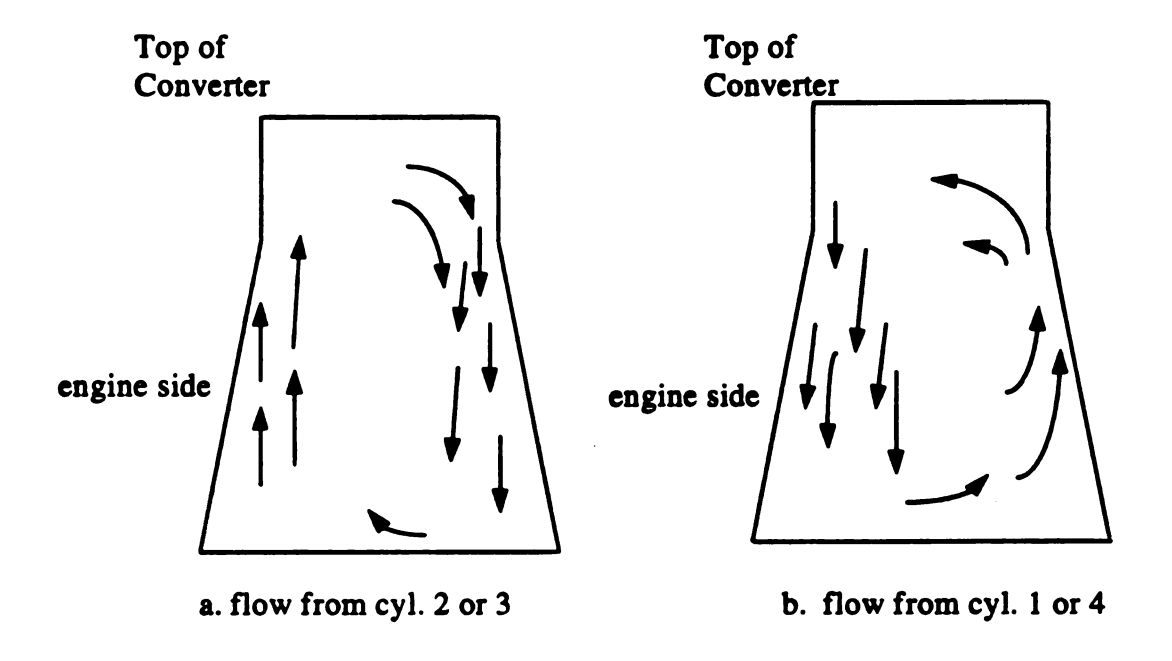


Figure 19. Schematic of intake and exhaust valve timing (0 degree stands for TDC of intake stroke)



## Minor axis flow visualization

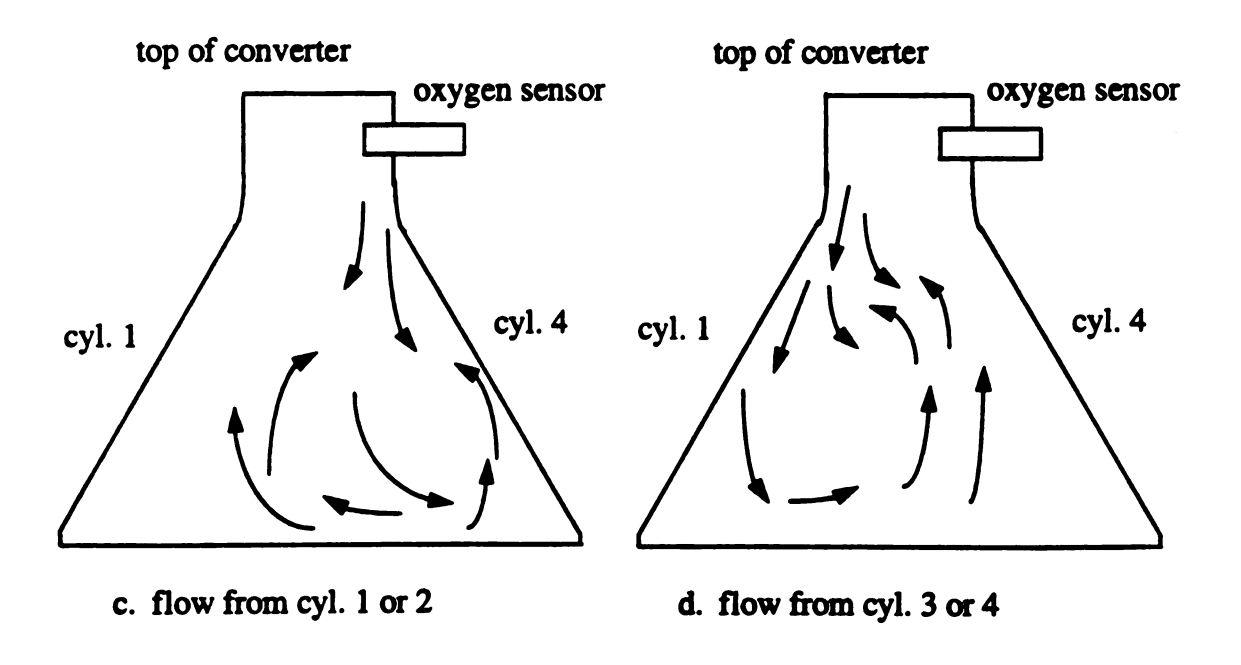


Figure 20. Sketches of flow patterns from the flow visualization films

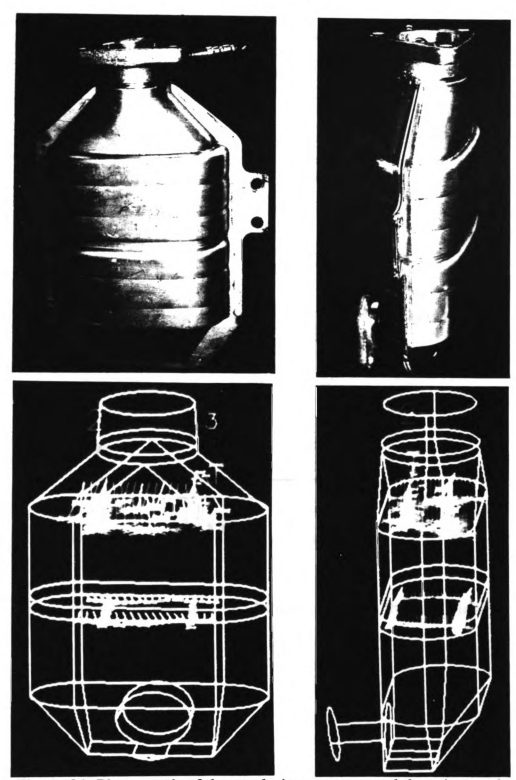


Figure 21. Photograph of the catalytic converter and the wire mesh model

- a. Front view of prodecution converter (top left)
- b. Side view of production converter (top right)
- c. Front view of wire mesh mode (bottom left)
- d. Side view of wire mesh mode (bottom right)

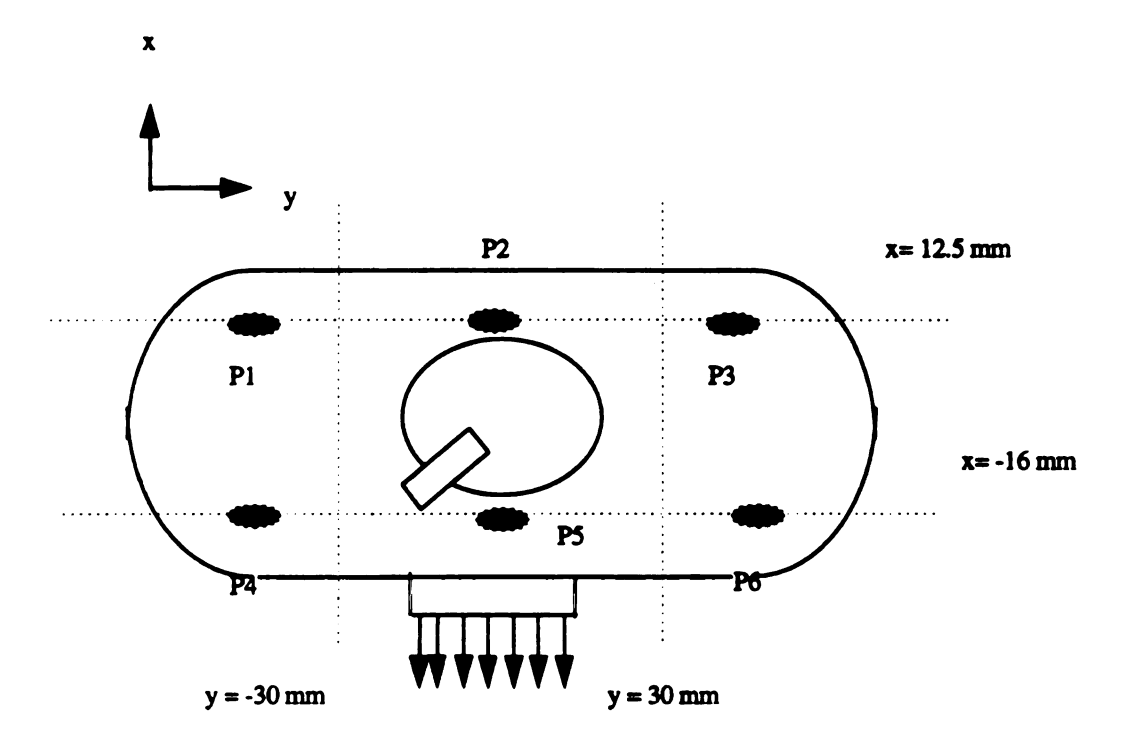


Figure 22. The location of the six points in the inlet plenum

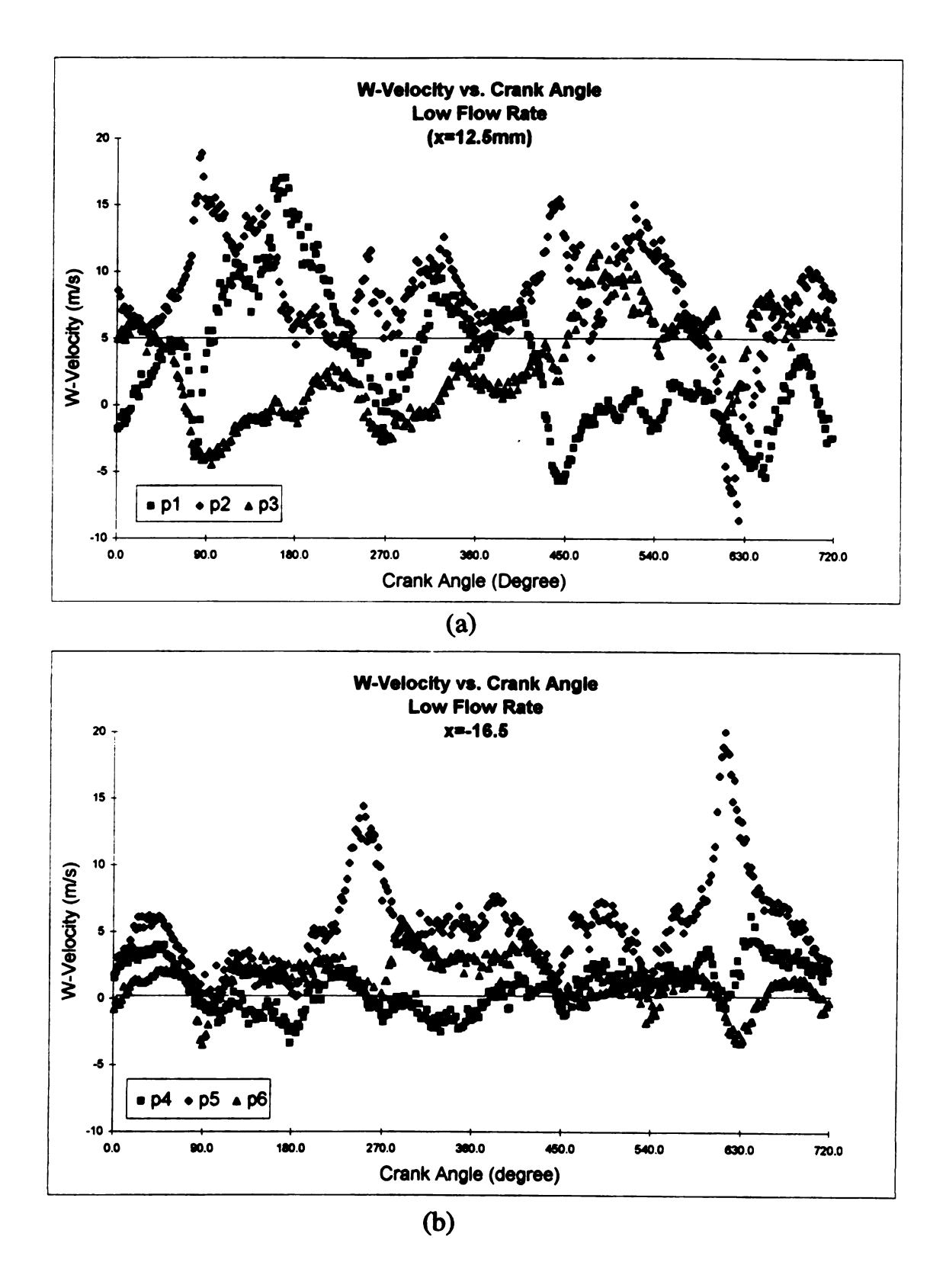


Figure 23. W-velocity vs. crank angle (a) low flow rate (b) high flow rate

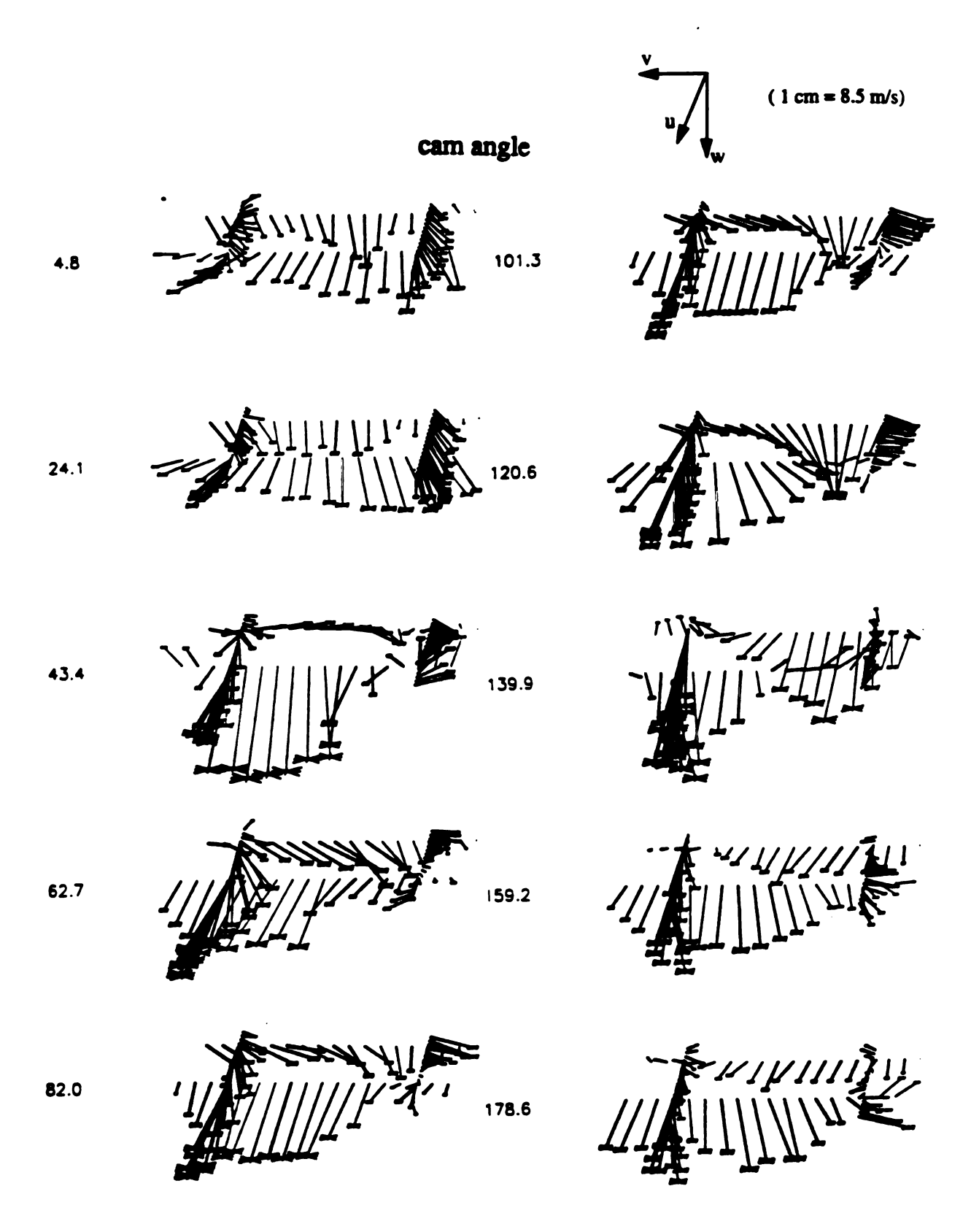
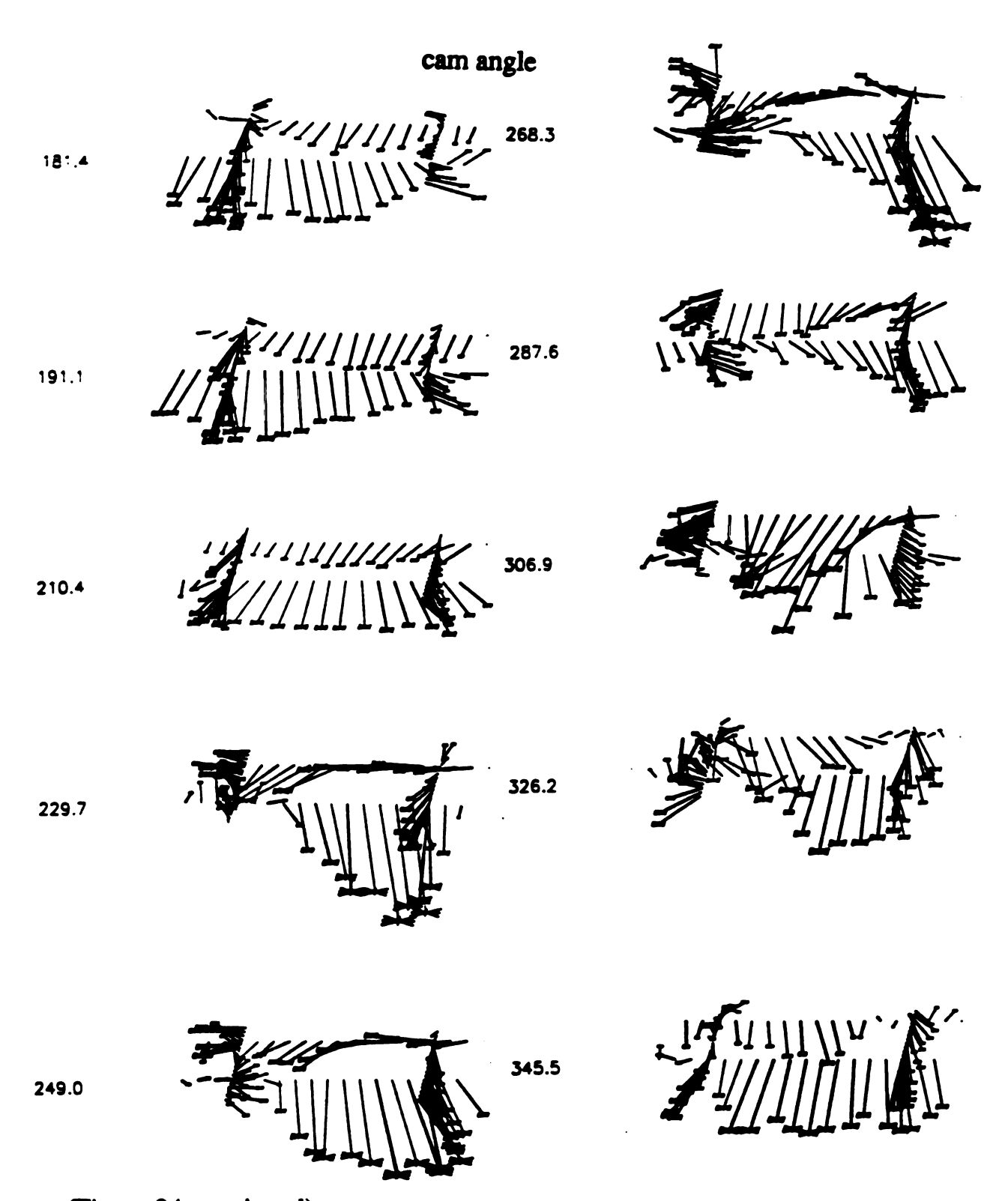


Figure 24. Animated inlet plane velocity profile with 120 scmh flow rate at engine speed 1000 rpm.



(Figure 24. continued)

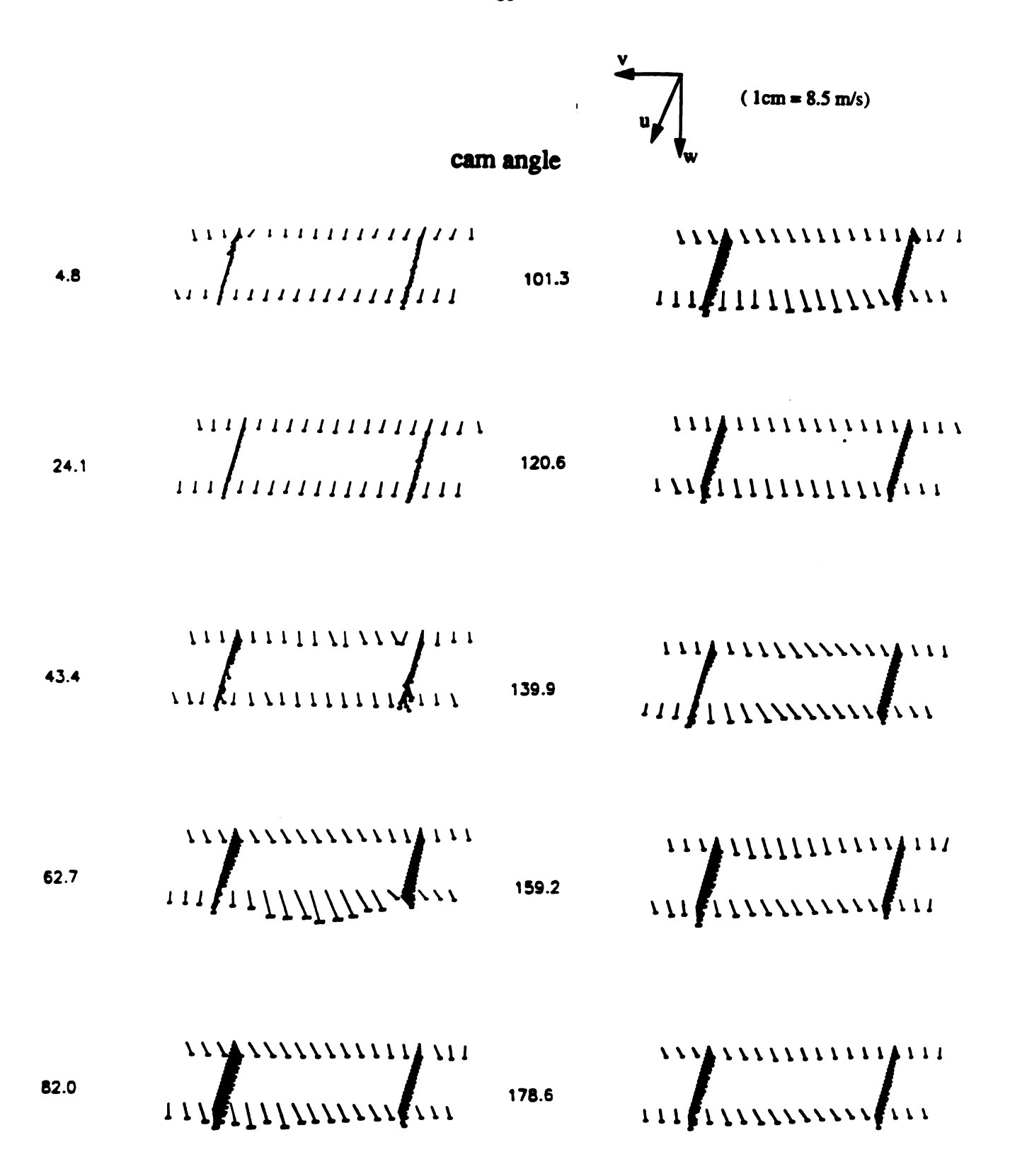


Figure 25. Animated midsection plane velocity profile with 120 scmh flow rate at engine speed 1000 rpm

## cam angle 268.3 181.4 191.1 210.4 229.7 249.0

(Figure 25. continued)

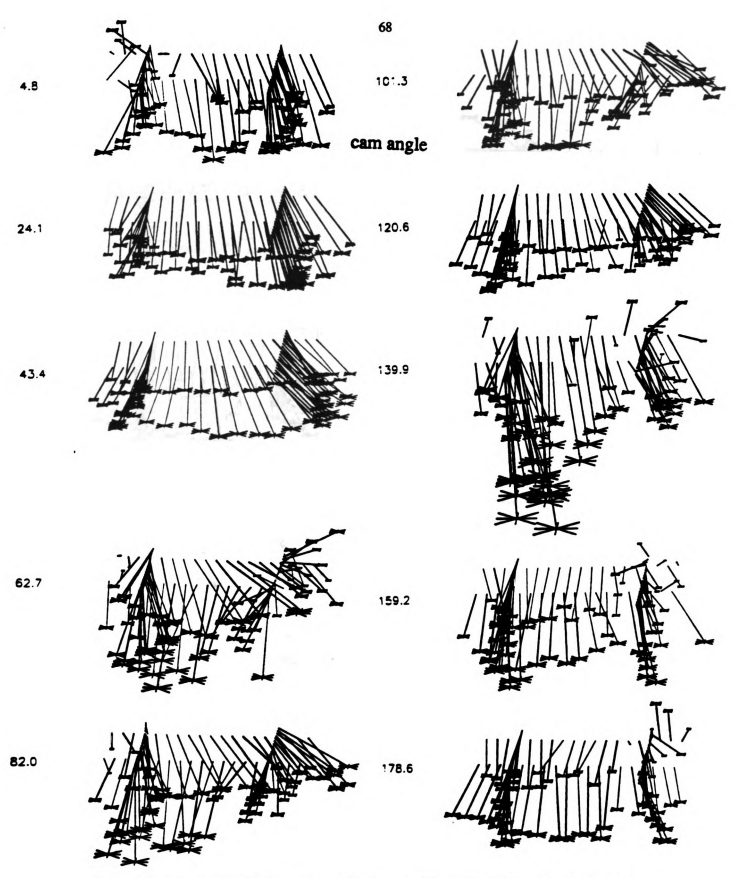
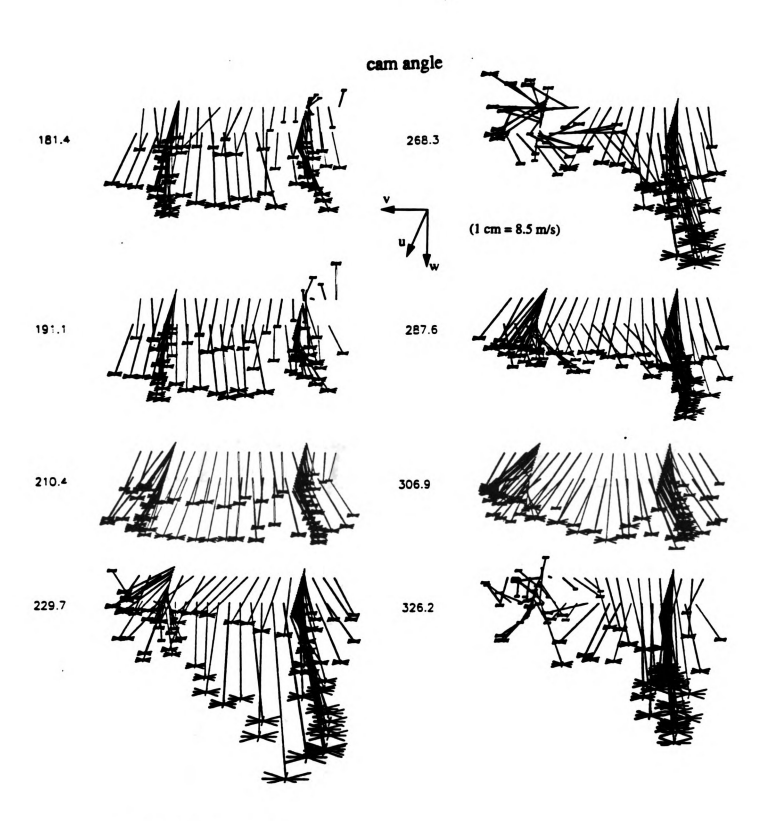


Figure 26. Animated inlet plane velocity profile with 205 scmh flow rate at engine speed 2000 rpm.



(Figure 26. continued)

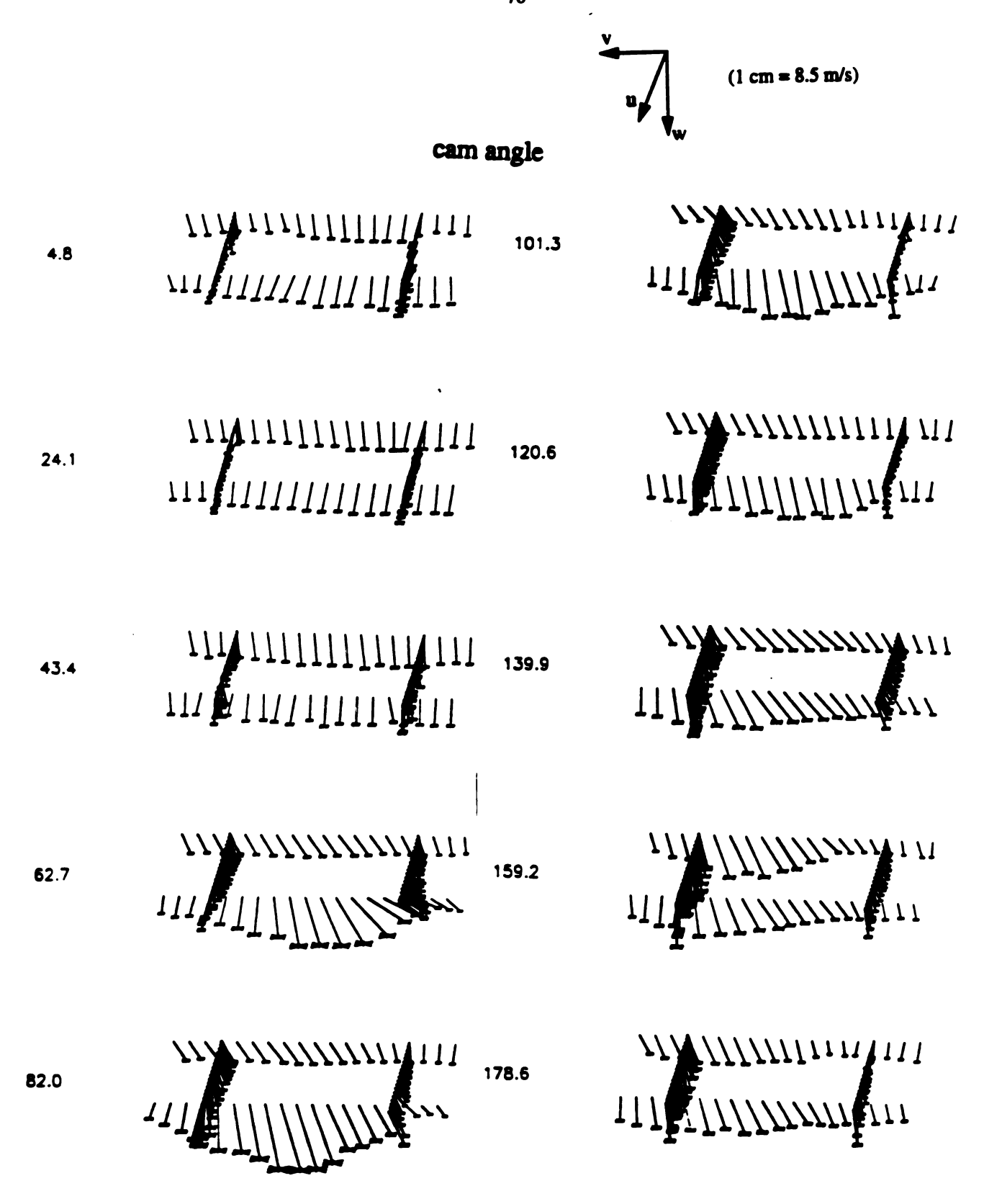
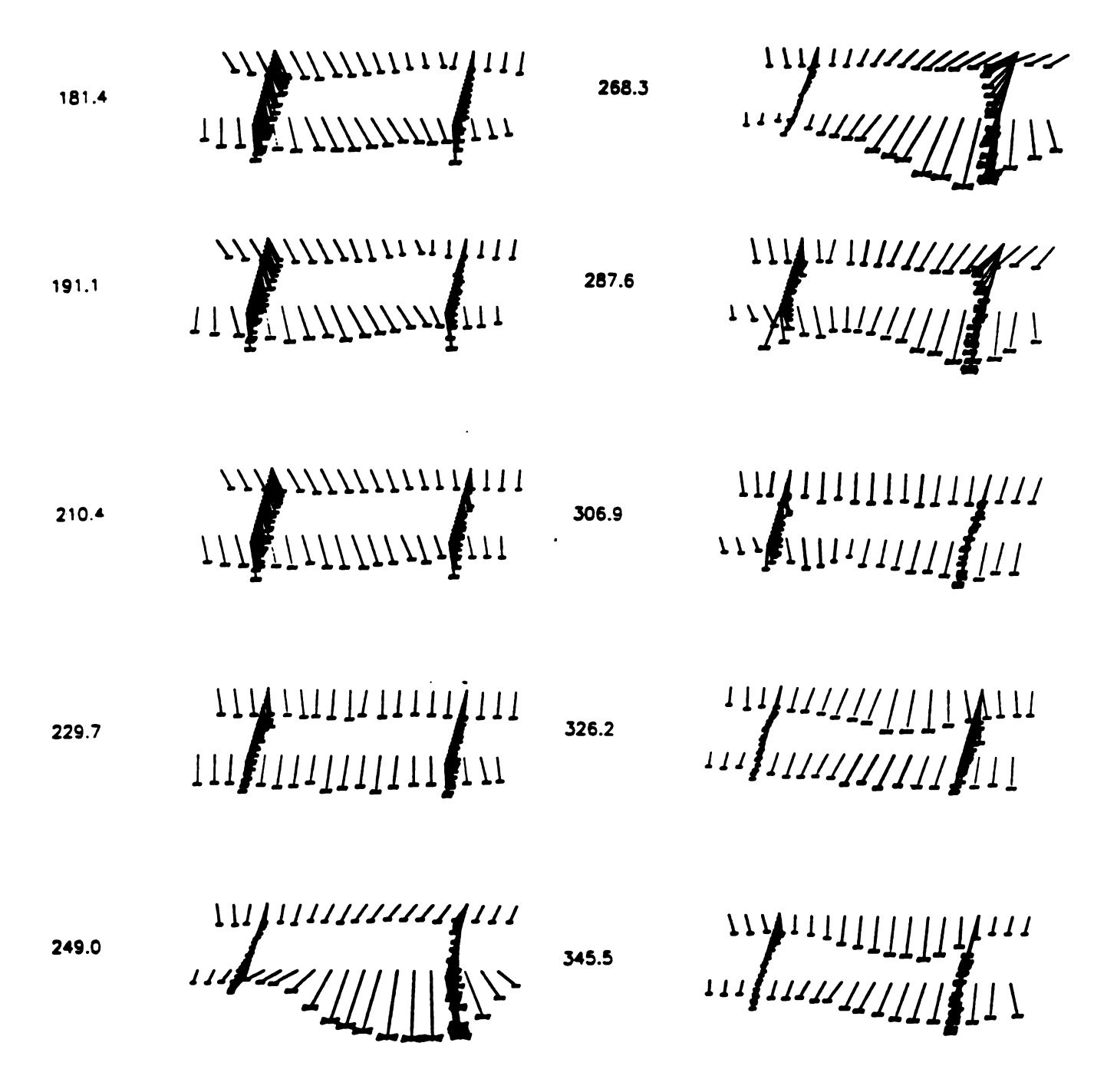


Figure 27. Animated midsection plane velocity profile with 205 scmh flow rate at engine speed 2000 rpm



(Figure 27. continued)

AICHIGAN STATE UNIV. LIBRARIES
31293013996677